APPLICATION OF STRUCTURAL DYNAMICS IN EARTHQUAKE AND WIND ENGINEERING

by

Benito M. Pacheco, D. Eng.*

ABSTRACT

Using minimal mathematics, extensive reference to the technical literature, and selected figures and tables, state-of-the-art concepts of structural dynamics are introduced as applied to seismic and wind-induced vibrations. Physical interpretations of mathematical concepts, and practical concerns of civil-structural engineer are emphasized. The presentation attempts to highlight some similarities and also sharpen certain contrasts between earthquake and wind effects.

INTRODUCTION

Applied Structural Dynamics

Structural dynamics, the theory, is a fusion of the well established theory of structures and theory of vibrations. In principle, the theory should apply equally well to time-dependent load or action of any origin. Among the examples of dynamic action that a civil-structural engineer is likely to encounter are: strong ground shaking due to earthquake or underground explosion; fluctuating wind pressure; moving load on bridge or building; operating machine; water waves on immersed structure; and accidental collision.

*Asst. Professor, Dept. of Civil Eng., Univ. of Tokyo, 7-3-1 Hongo, Tokyo 113

In practice, however, concepts of structural dynamics are usually applied with further approximations and simplifications that are justifiable, perhaps restrictedly, for the particular dynamic load or loads under consideration. In the first place, manageable dynamic analysis allows less detail in the structure model than would be usual for static analysis. Moreover, the simplest reasonable model has to be used in the description of the dynamic load, if the analysis of the dynamic response is to remain tractable. The approach is herein termed as applied structural dynamics.

This paper (abridged and updated from Ref. 1) reviews concepts of applied structural dynamics as commonly used in the analysis of vibrations due to earthquake and wind. The civil-structural engineer is most likely to compare, if not liken, these two dynamic actions because both are widely recognized sources of so-called lateral forces, i.e. horizontal forces that are perpendicular to the main axis of the structure. The two types of dynamic action can be more accurately compared and differentiated from the viewpoint of applied structural dynamics.

Outline

The first part of this paper is concerned with the modelling of structure and identification of dynamic properties. Analytical, experimental and empirical methods are mentioned. Natural period of vibration and subcritical viscous damping are discussed from both physical and mathematical viewpoints. Modes of vibration are introduced in the physical sense. It is subsequently pointed out that these dynamic properties of structure may in reality change with time.

The modelling of earthquake or wind action is discussed in the second part, under the assumption that interaction with the vibrating structure may be ignored. While certain spatial characteristics are mentioned, emphasis is on temporal properties as these compare to structural vibration period(s) and design lifetime. Time as physical parameter takes central role in three major ways. First, the dominant period of fluctuation of earthquake or wind force may or may not coincide with a natural period of the structure, accordingly changing the type of dynamic response from resonant to nonresonant.

Second, the duration of the load or action may be short or long compared to structural natural period(s), accordingly requiring the engineer's attention to either the peak of transient vibration or the amplitude and number of oscillation cycles. Third, the return period, i.e. statistically expected time interval between two occurrences of same-intensity earthquake or wind, may be short or long relative to the expected or design lifetime of the structure, thereby dictating the extent of local structural damage that may be deemed tolerable and repairable in between. Choice of structural system at design stage, as influenced by this third time factor, determines whether the structure itself by design will have some properties significantly varying with time.

Vibration of the structure, or its mere existence in its specific size and form, may yet alter the effective action of earthquake or wind from estimates based on measurements at, or analyses of, the site without the structure. Interaction between structure and surrounding medium is subsequently discussed in brief.

Lastly, as the engineer's ultimate objective in analyzing vibration in his structure is to prevent or suppress it, this paper closes with a discussion of modern concepts of vibration isolation, damping, and active control.

Table 1. Main Types of Full-Scale Test

A. Free vibration
   1. Initial displacement ("pull-back")
   2. Initial velocity ("impulsive")

B. Forced excitation
   1. Steady-state sinusoidal
   2. Variable-frequency sinusoidal ("run-down")

C. Transient disturbance
   1. Short-duration mechanical excitation
   2. Ambient/Microtremor
   3. Blasts
   4. Wind
   5. Earthquake

D. Pseudo-dynamic test

E. Shaking Table test

SYSTEM IDENTIFICATION

Full-scale testing

Table 1 is a modification and update of the classification given in Ref. 2 of dynamic tests and observations of full-scale structures and models. Despite extensive experimental research and testing of structural components, techniques of synthesis of data so obtained have not in any significant way lessened the need for testing of full structures.

In a full-scale test, the engineer's likely intention is not merely to observe the overall dynamic characteristics, but also to calibrate a model, which may be mathematical or experimental. The basic idea of system-model "identification" is outlined in Fig. 1. Path (a)-(b) represents the test; path (c)-(d)-(g) is the completion of system-model identification; and loop (d)-(e)-(f) is the iterative search for appropriate values of the system-model parameters. Path (h)-(i) in the lower part of Fig. 1, is the intended use of identified system model. Theories and techniques for system identification in structural dynamics are presently under extensive research [e.g. Refs. 3-4].

Natural period and viscous damping

Following is a discussion of possibly the simplest examples of system identification. They are the simplest because: 1) the models to be suggested are the simplest know; and 2) the test principles are straightforward. Figure 2(a) schematically shows a pull-back free-vibration test (Item A-1 in Table 1) of a steel stack. The history of displacement in this case (Fig. 2(b), may acceptably be modelled by a smoothed-out "record" as in Fig. 2(c), as overall discrepancy becomes "negligible".

The record in Fig. 2(c) may be obtained by adopting and calibrating the following model: linear, subcritical viscously damped, single-degree-of-freedom (SDOF) oscillator (Fig. 3). This model as represented by mechanical elements, assumes that the equivalent spring constant k, dashpot constant c, and mass m are positive time-invariant quantities.

In the absence of external excitation force, i.e. in free vibration, dynamic equilibrium is attained among the spring force (-kx), dashpot force (-cẋ), and inertia force (-mẍ). (See Fig. 4.) Equations (1)-(3) below are simply alternate ways of stating this dynamic equilibrium. It is known mathematically that if $x(t=0) = x_0 \neq 0$ and $x(t=0) = 0$ as in pull-back test, then Eq. 4 is a solution of Eq. 3:

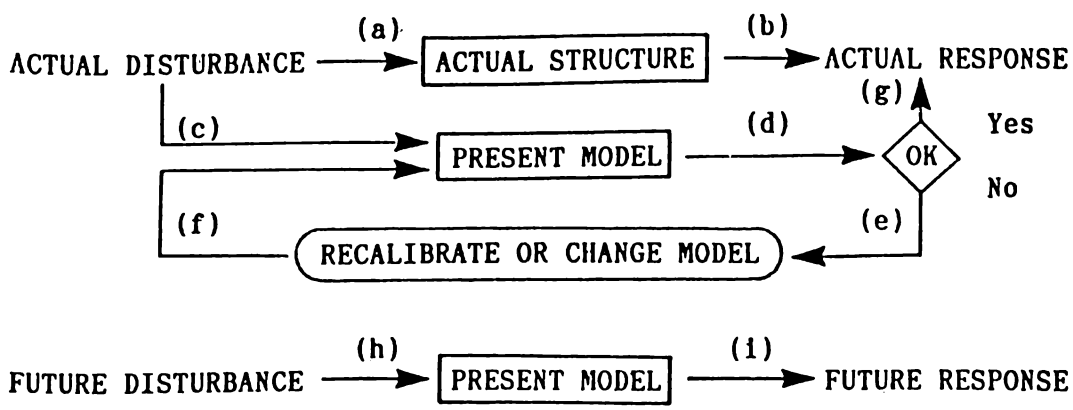

Figure 1. Basic idea of system-model identification

$$m\ddot{x} + c\dot{x} + kx = 0 \qquad (1)$$

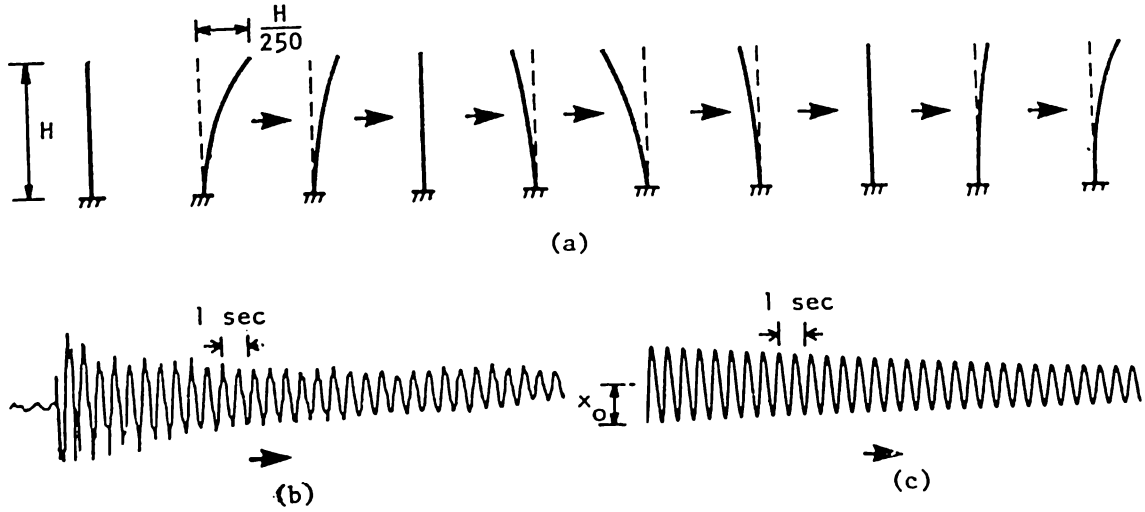

Figure 2. Example of pull-back test. (a) "Snapshots" of one "cycle" of free vibration of 110-ft-high stack (showing only its center line; scale of displacement is greatly enlarged for clarity). (b) Time record of displacement of a point about 12 ft from the base. (c) A smoothed-out version of (b).

$$\ddot{x} + \frac{c}{m}\dot{x} + \frac{k}{m}x = \frac{0}{m}, \qquad m \neq 0 \qquad (2)$$

$$\ddot{x} + \frac{4\pi\xi}{T}\dot{x} + \frac{4\pi^2}{T^2}x = 0 \qquad (3)$$

$$\xi = \frac{c}{2\sqrt{km}} \text{ (dimensionless)}; \quad T = 2\pi\sqrt{m/k} \text{ (time)}, \; k \neq 0 \qquad (3a), (3b)$$

$$x(t) = (x_0)\left(e^{-\frac{2\pi\xi}{T}t}\right)\left(\cos\left[\left\{\frac{2\pi\sqrt{1-\xi^2}}{T}t\right\} - \left\{\mathrm{Tan}^{-1}\frac{\xi}{\sqrt{1-\xi^2}}\right\}\right]\right) \qquad (4)$$

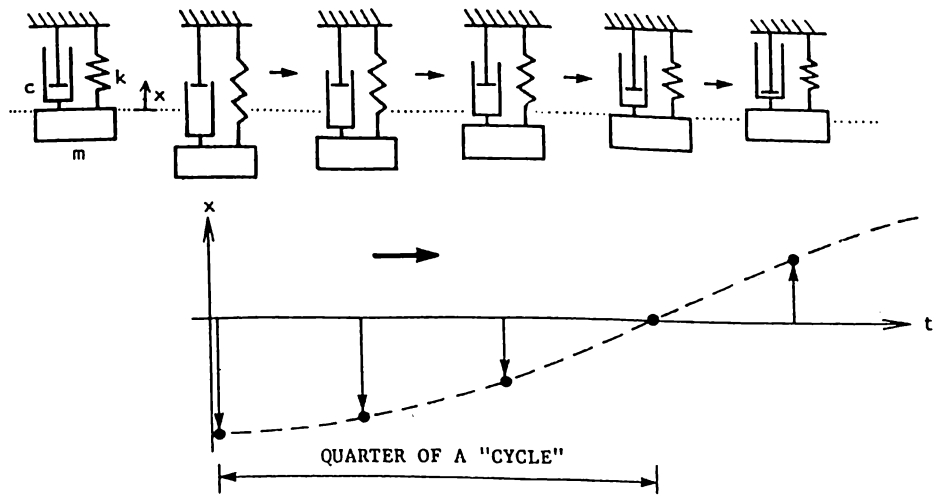

Figure 3. "Snapshots" of SDOF oscillator model during free vibration, and plot of oscillator displacement, x, versus time, t

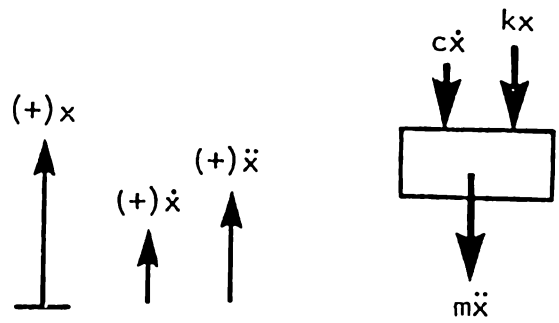

Figure 4. Definition of positive direction for displacement x, velocity $\dot{x}$, and acceleration $\ddot{x}$. Also showing forces in dynamic (instantaneous) equilibrium.

Using Eq. 4 with calibrated parameters T = 0.645 sec and ξ = 0.004, and initial displacement x_o as indicated in Fig. 2(b), the time history in Fig. 2(c) may be reproduced. In the terminology of system-model identification, if this is acceptable as reproduction of actual record (Fig. 2(b), then a linear SDOF model with parameters T = 0.645 sec and ξ = 0.004, has been identified for the stack. Figure 5 illustrates why T is referred to as natural period of the structure, i.e., $T_D \cong T$ is the period of free or natural oscillation about the static equilibrium ($x = 0$) position.

The oscillation is not periodic in the mathematical sense, however, since the peak amplitude at each "cycle" is not equal but slightly smaller than that at the preceeding "cycle". Such oscillation is "damped", and ξ is the damping ratio. (The term "ratio" is suggested by Eq. 3a, where ξ is the ratio of dashpot coefficient c and the quantity $2\sqrt{km}$. The displacement due to initial disturbance shall be oscillatory provided the ratio ξ is less than unity.) The smooth curve enveloping all the positive peaks, is neither straight nor horizontal but decreases with progressing time at an exponential rate proportional to ξ.

The parameters T and ξ may also be identified by steady-state sinusoidal force vibration (Item B-1 in Table 1), which is another conceptually simple test. In terms of the mechanical model (Fig. 6(a), this means applying a sinusoidal periodic force with amplitude p_o and frequency f, from rest condition. The time history of displacement may look like Fig. 6(b). If such test is repeated with the same force amplitude p_o but different frequency f, and the steady-state displacement amplitude x_S is plotted against f, a graph like Fig. 7 may be obtained, from which T and ξ may be calculated as indicated.

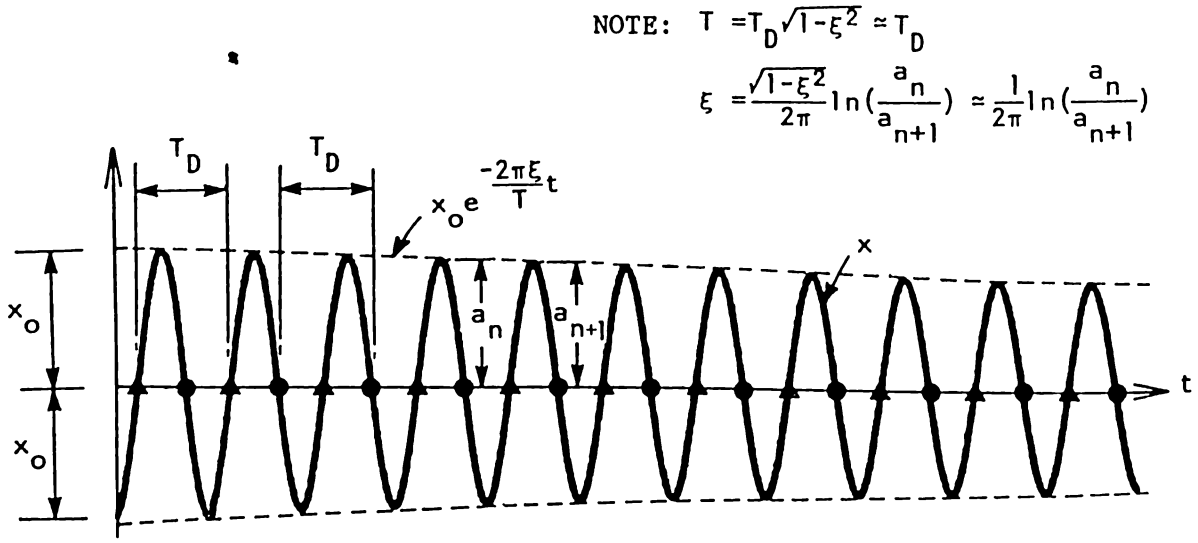

Figure 5. Enlarged copy of Fig. 2(c) in elongated time scale, showing: period TD between two successive "positive zero crossings" (▲) or "Negative zero crossings" (●); and envelope curve (----) enveloping all positive peaks.

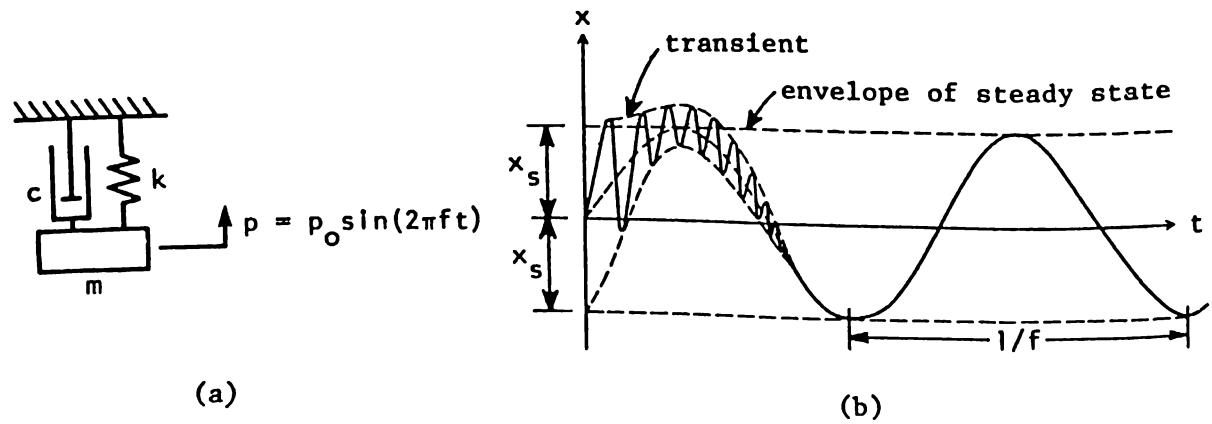

Figure 6. (a) SDOF system with sinusoidal excitation force. (b) Forced displacement response of hypothetical case with rather high damping ξ, and excitation force period much longer than natural period ($T_E = 1/f >> T$).

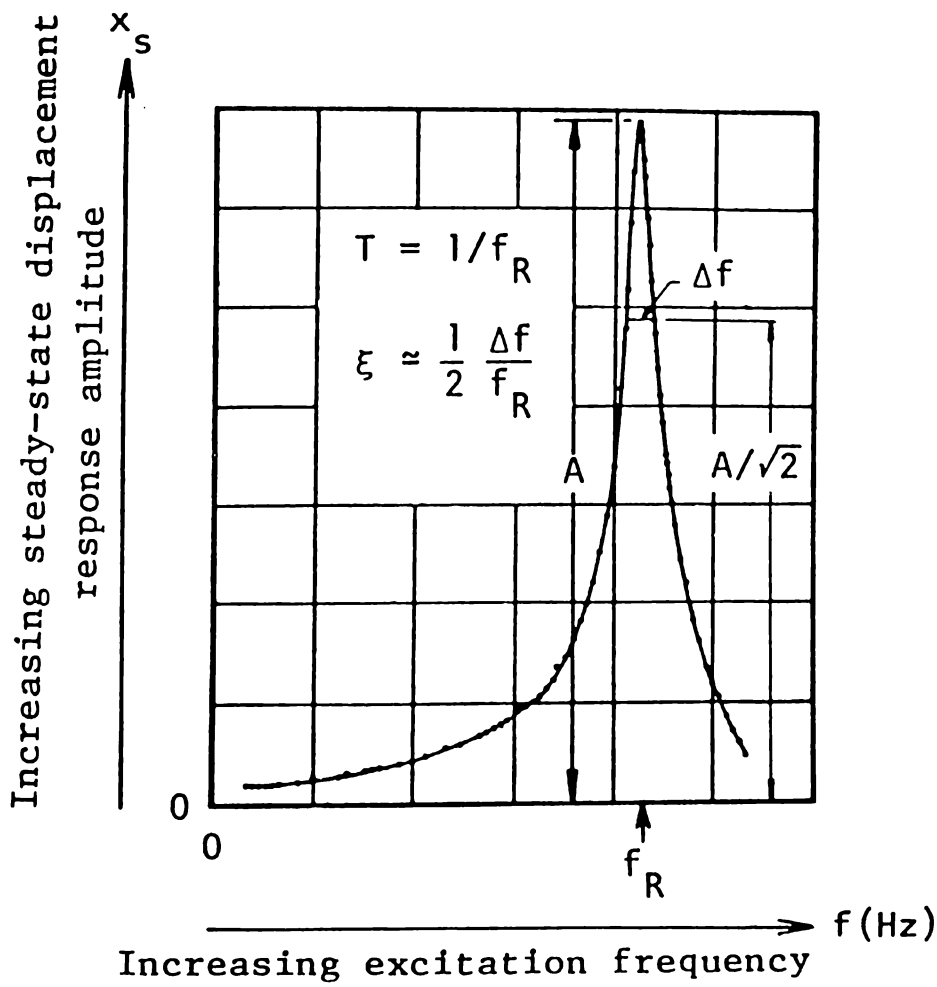

Figure 7. Form of data from steady-state sinusoidal forced excitation test to identify parameters of linear SDOF model (Note: Hz = cycle per second)

The significance of natural period T and damping ratio ξ as dynamic properties of the structure, may be summarized by referring to Fig. 8. First note that $x_{st} = (p_o/k)$ would be the displacement if a static force p_o was applied. When a sinusoidal force is applied very gradually, i.e., with frequency much lower than resonant frequency f_R or period much longer than T, the amplitude of oscillatory displacement would not be drastically different from x_{st}. This range (of low excitation frequency or long period) may be called pseudo-static. In the other extreme, the displacement amplitude would be nearly zero if the frequency of force was extremely high or the excitation period was very short compared to T. In this range, which may be called inertial, the inertia force effectively cancels the excitation force.

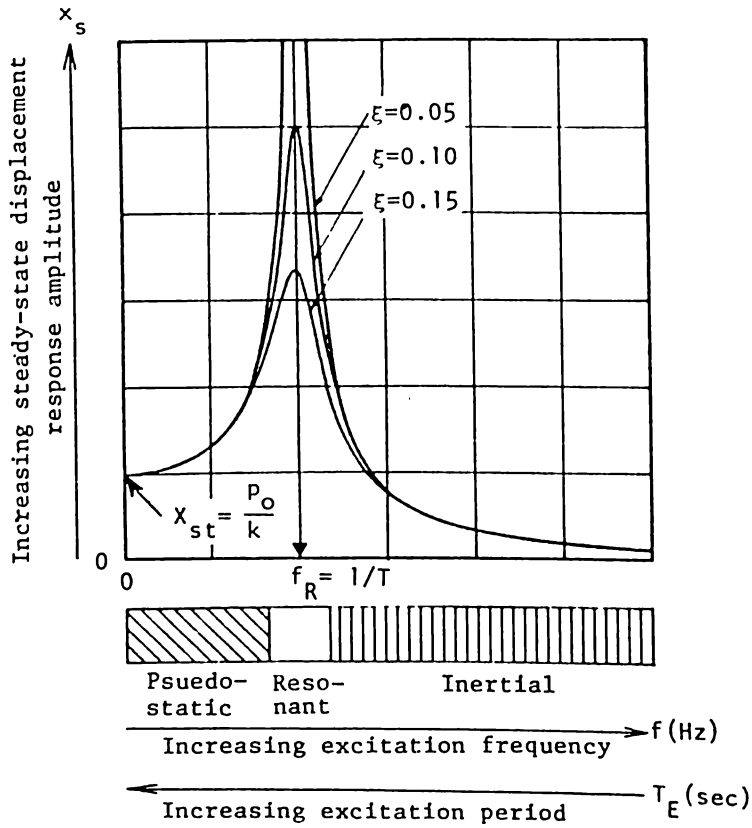

Figure 8. Displacement-frequency response plots for fixed natural period T and three different values of damping ratio ξ, showing pseudo-static, resonant, and inertial ranges of steady-state sinusoidal excitation.

Between the two extremes just mentioned is the resonant range, where the displacement response may be very large when the damping ratio is very low. In this range the damping plays a very crucial role in reducing the amplitude of oscillatory displacement. It is known mathematically that for given T, ξ , and p_o in Eq. 5,

$$\ddot{x} + \frac{4\pi\xi}{T}\dot{x} + \frac{4\pi^2}{T^2}x = (p_o / m) \sin(2\pi ft) \qquad (5)$$

the maximum possible displacement amplitude is related to ξ as:

$$x_{\text{max. pos.}} = x_{st}\frac{1}{2\xi\sqrt{1-\xi^2}} = x_{st}\frac{1}{2\xi} \qquad (6)$$

and this is attained when the excitation period ($T_E = 1/f$) is $T_E = \frac{T}{\sqrt{1-2\xi^2}} \cong T$ the condition of so-called resonance. For example, the magnification factor $1/2\xi$ is as large as 50 when ξ is 1%, values not a typical of modern conventionally constructed structures.

Multiple modes

It has been implied in the discussion so far that one displacement, i.e. x(t) is enough to fully describe the time-varying configuration of the structure. The snapshots in Fig. 2(a), for example, show the stack vibrating in essentially constant shape, with time-varying amplitude. When steady-state sinusoidal forced excitation is performed on this stack (e.g. by a sinusoidal horizontal force applied at 12-ft elevation), and experimental data points are plotted as in Fig. 7, it may be verified that the data points clustering around the sharp peak are corresponding to essentially the same shape of vibration.

The usual procedure in this type of forced excitation test is to start with a low frequency and repeatedly obtain data points (i.e. pairs of f and x_S) by slightly increasing this frequency each time, until the peak around resonant frequency, f_R shall have been located. In actual structures, however, if sufficiently high frequencies can be covered as well in the "frequency sweep", it is possible to locate higher resonant frequencies. An illustrative example is given below.

In Fig. 9(a), a building frame whose floor and roof systems are relatively heavy and rigid, and the columns are rather light, is excited by a sinusoidal force at the roof level. The steady-state displacement amplitude at each level (1, 2 or 3) is recorded, non-dimensionalized by division with static displacement due to a static force p_o at the roof level, and plotted against excitation frequency in Fig. 9(b). As a wide spectrum of frequency is covered, not only one but three resonance peaks are located that are quite distinct from each other, at frequencies f_{R1}, f_{R2} and f_{R3}.

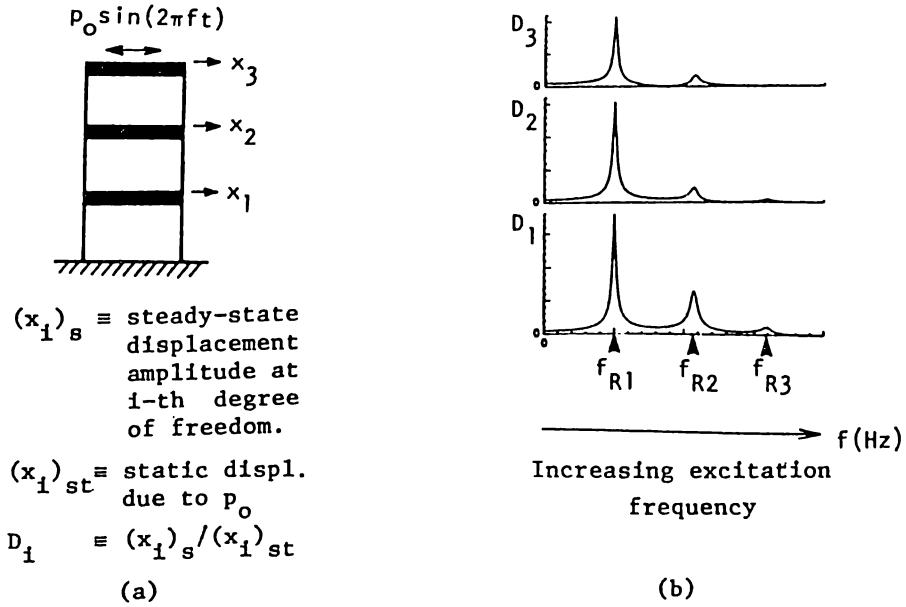

Figure 9. (a) Building frame subjected to sinusoidal force at roof level. (b) Non-dimensionalized displacement-vs-frequency response plots for three degrees of freedom, covering a wide spectrum of excitation frequency and locating three resonant frequencies. [Adapted from Ref. 5]

An inspection of the simultaneous time histories of displacements x1, x2 and x3, may reveal that they are related as in Fig. 9(c) for $f = f_{R1}$. The column vector $< x1(t)\ x2(t) >^T$ defines a vibration shape labeled as $\Phi 1$, the so-called fundamental mode. The associated resonant frequency f_{R1} is regarded as fundamental natural frequency; T_1, as fundamental period. Figures 9(d) and 9(e) demonstrate the other modes $\Phi 2$ and $\Phi 3$, corresponding to higher resonant frequencies or shorter natural periods.

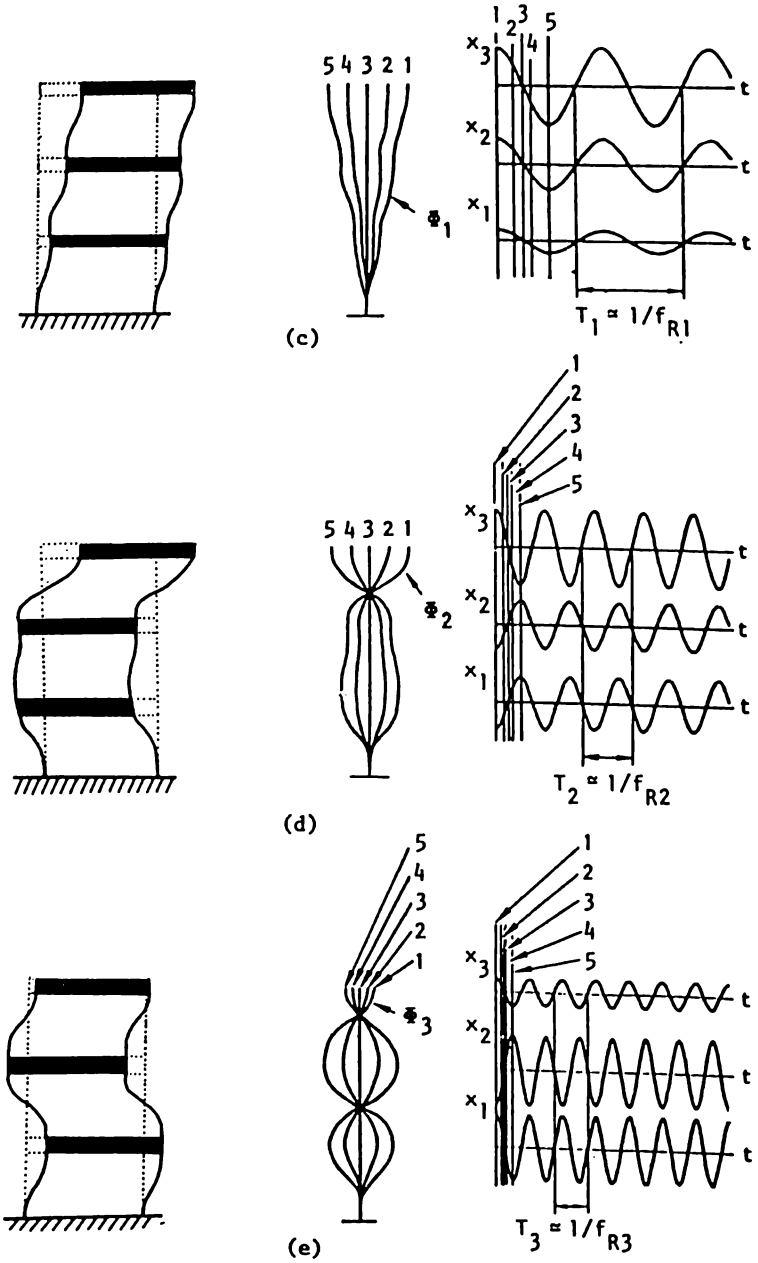

Figure 9 (Continued). Mode shapes and segments of displacement histories of three degrees of freedom, at steady state. (c) Mode 1. (d) Mode 2. (e) Mode 3. (Note that the displacements are shown in extremely exaggerated scale.)

Each resonant region in Fig. 9(b), when separately drawn to appropriate scale, resembles the resonant range in Fig. 7, indicating that the natural period and damping ratio of each mode may be calculated similarly.

The three-story frame discussed above, or any structure that displays more than one resonant region within the frequency range of interest, has to be modelled as a multi-degree-of-freedom (MDOF) system. The necessary mathematical model involves simultaneous differential equations in **n** unknowns or degrees of freedom, e.g. displacements $x1(t)$, $x2(t)$, ..., $xj(t)$, ...,$xn(t)$, where some x's may be rotational instead of translational displacements. The coupled differential equations may be written in matrix form, analogous to Eq. 5, as:

$$M\ddot{x} + C\dot{x} + Kx = p \sin(2\pi ft) \qquad (7)$$

where $x = < x1(t)\ x2(t) \ldots xj(t) \ldots xn(t) >^T$; **M** is matrix of mass or inertia coefficients; **C** is matrix of dashpot or damping coefficients; **K** is matrix of spring or stiffness coefficients; and **p** is load distribution vector. For the frame in Fig. 9, these matrices and vectors are of the following forms:

$$\mathbf{x} = < x_1(t) \quad x_2(t) \quad x_3(t) >^T$$

$$\mathbf{p} = < 0 \quad 0 \quad p_0 >^T \qquad \mathbf{M} = \begin{bmatrix} m_1 & 0 & 0 \\ 0 & m_2 & 0 \\ 0 & 0 & m_3 \end{bmatrix}$$

$$\mathbf{C} = \begin{bmatrix} c_1 + c_2 & -c_2 & 0 \\ -c_2 & c_2 + c_3 & -c_3 \\ 0 & -c_3 & c_3 \end{bmatrix} \qquad \mathbf{K} = \begin{bmatrix} k_1 + k_2 & -k_2 & 0 \\ -k_2 & k_2 + k_3 & -k_3 \\ 0 & -k_3 & k_3 \end{bmatrix}$$

Coefficients of mathematical model

Calibration of parameters m, c and k, or **M**, **C** and **K** in MDOF system is, in principle, possible from resonance characteristics as determined from vibration test. However, whereas the parameters **T** and ξ are enough to define the resonance characteristics of SDOF system, an additional information is necessary before all three unknowns, m, c and k, can be calibrated using Eqs. 3(a) and (b). It is common in practice to deduce **k** separately from static loading (i.e. k = static force divided by static displacement in the direction along the force), or estimate the equivalent mass separately. Similarly, information in addition to mode shapes, modal periods and modal damping ratios, are required before **M**, **C** and **K** can all be calculated [e.g. Ref. 6, Appendix 1].

In fact, for analytically estimating **k** or elements of **K**, many analytical techniques are available that are direct extensions of static structural analysis. Meanwhile, m or **M** may be approximated by assuming the structural mass to be divided into lumps at specified locations, or by use of "mass-consistent finite elements" [e.g. Ref. 7].

Coefficient **c** or **C** is by far the most difficult to estimate theoretically [e.g. Ref. 8]. At least two reasons may be cited why such difficulty has been too often deemed unnecessary. Firstly, there is a lingering doubt that viscous damping (as represented by the term $\mathbf{C}\dot{\mathbf{x}}$ in Eq. 7) is as realistic as it is simple, given the acknowledged complexity of energy dissipation mechanism in real structures. Secondly, as suggested by Fig. 8, damping is thought to be crucial only in resonant steady-state excitation. Nevertheless, viscous damping remains practical as model, and it has been suggested that damping coefficients be identified from full-scale test data [e.g. Ref. 9]. At design stage, however, all parameters anyway must be estimated theoretically or empirically.

Empirical formulas

Theoretical and empirical methods of estimating dynamic structural parameters are indeed also necessary. Full-scale tests, while most desirable, are frequently difficult to implement even when the structure is already existing. In general, to observe each one of several modes of a complex structure in free vibration, a complicated combination of initial displacements and velocities have to be applied. On the other hand, in steady-state forced vibration, one or more large exciters and huge amount of mechanical energy input may be necessary. In both tests, a prior knowledge of the vibration shape may be crucial in situating the test instruments, making the procedure essentially iterative. On top of such problems in instrumentation, it is possible that two or more structural modes may have nearly equal periods. Or, the structure may not have modes in the sense of different points in the structure oscillating in synchronization, as can happen when the damping distribution in the structure is of the so-called non-proportional type. The data processing may become complicated, or completely erroneous, should the implicit mathematical model be very different from measured behaviour [e.g. Ref. 9]. Other types of test (e.g. Transient disturbance or Items C in Table 1) may take advantage of naturally or easily generated disturbances, but nevertheless face difficulties in data processing or reduction.

Due to these and other practical difficulties, very few statistical analyses of natural period and damping ratio of existing structures can be found in the literature. Some available empirical formulas and "typical" values are summarized below.

Figure 10 shows "representative" values of fundamental natural period. For buildings, seismic design codes suggest approximate empirical formulas, as listed in Table 2. The subject of damping has been more complicated. Early on, investigators have concluded that there are various physical mechanisms of energy dissipation, i.e. damping, in actual structures, and viscous

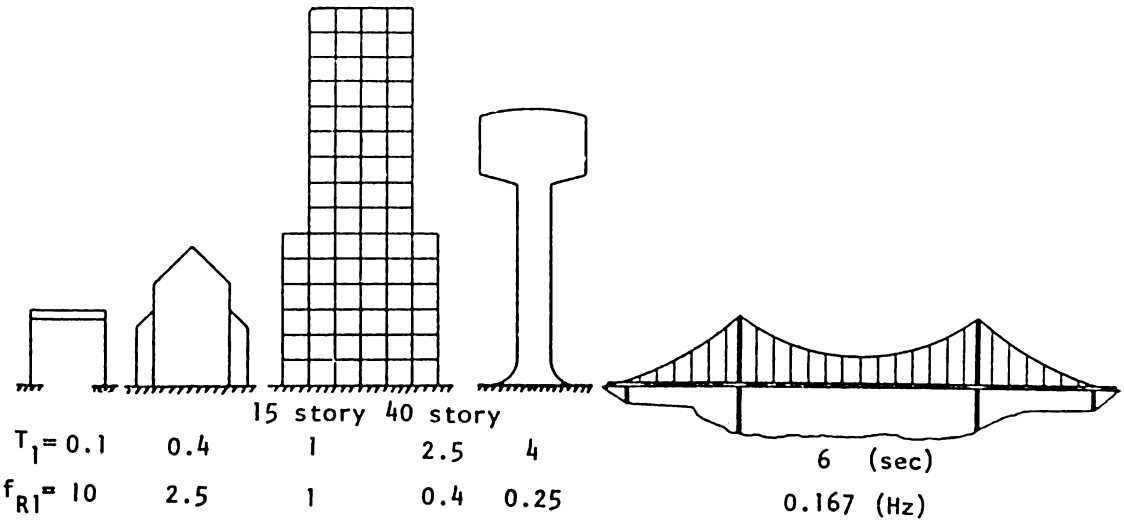

Figure 10. "Typical" fundamental period of selected types of structures [After N.M. Newmark]

damping is but an "equivalent" form Test data on equivalent damping ratio have indeed shown large scatter, and some investigators have tried to correlate the data with such parameter as representative dimensions of structure, natural period, and amplitude of oscillation. A recent study [Ref. 12] of nine tall buildings (base dimension ranges 12 - 50 m) yielded the following empirical formula for damping ratio in j-th mode:

$$\xi j = (46 + 10^{0.5\sqrt{D}} x_{Hj} \quad / H \qquad \text{(percent)} \qquad (8)$$

where H = height; D is overall dimension at the base, measured along the direction of motion; and x_{Hj} is either the steady-state displacement amplitude or 1/3 of maximum transient displacement at height H in mode j. (All lengths are in meters.) Data on bridges which were analyzed in an early study [Ref. 13] are summarized in Table 3 and Fig. 11.

Table 2. Empirical formulas for fundamental period of building

Reference	Building type	Approx. period (sec.)*
Ref. 10 (UBC-82) p.51; lengths in ft	Ductile frames Others	0.10 N 0.05 H / $\sqrt{D}$
Ref. 10 (ATC 3-06) p.73; lengths in ft	Steel moment-frames Concrete m-frames Others	0.035 H $^{0.75}$ 0.025 H $^{0.75}$ 0.05 H / $\sqrt{D}$
Ref. 11 (Japan) lengths in m	General	(0.02 + 0.01 p) H

*N=number of stories; H=height; D=overall dimension of floor plan at ground level, measured along the direction of vibration; p=ratio of the total height of stories of steel structure portion to the height of the building

Table 3. "Standard" values of damping ratio ξ for bridges [Ref. 13]

	Average	Minimum
Superstructure in vertical vibration		
Suspension and cable-stayed bridges (same for torsional vibration)	0.009	0.005
Other types with span > 40 m	0.013	0.005
Other types with span < 40 m	0.016	0.005
Whole bridge system in horizontal vibration		
Bridges on short piers (T=fund. period, sec)	0.02/T	0.01/T
Bridges on piers taller than 25 m	0.018	0.01

Nonlinearities

Actual buildings and bridges, as designed and built, are acceptably linear during small-amplitude ambient vibrations or microtremors, and even during mild wind or earthquake. In the corresponding mathematical models, m, c, k, or **M**, **C**, and **K** would be constants.

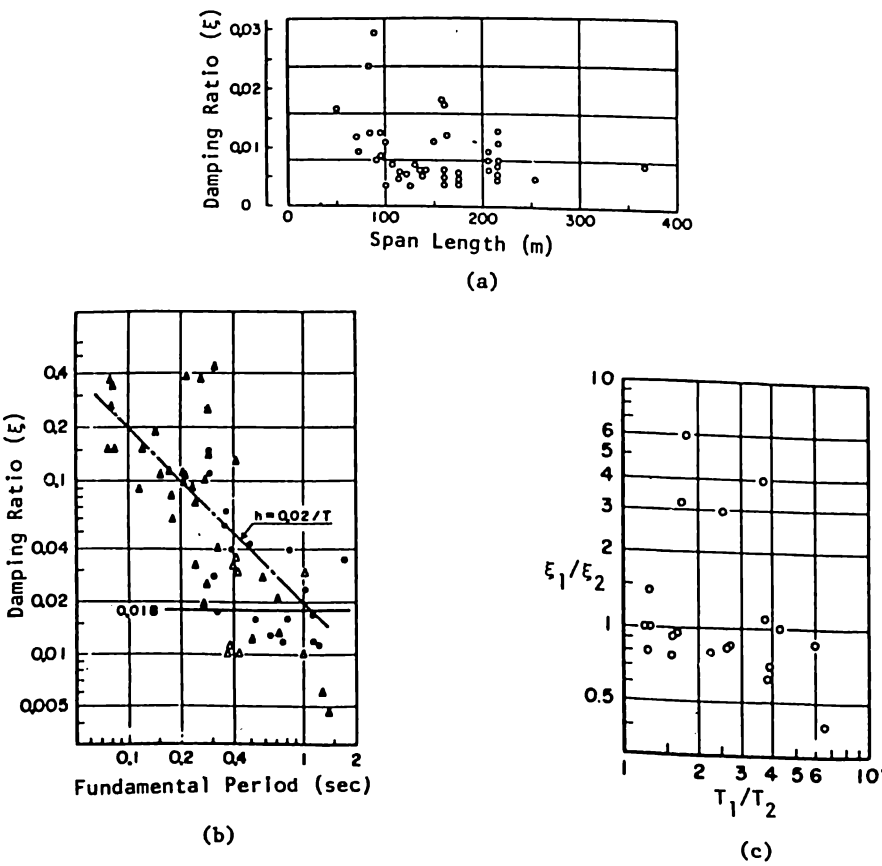

Figure 11. Test data on damping of bridges [Ref. 13]. (a) Damping of suspension and cable-stayed bridges vs. span length. (b) Damping vs. fundamental period in horizontal vibration for foundation and ordinary piers (▲); bridges and ordinary piers (●); tall piers with height greater than 25 m (Δ); and bridges on tall piers (○). (c) Comparison of damping ratios and natural periods of lowest two modes.

At larger amplitudes of vibration, however, several factors can change the "effective" linear parameters (or, more accurately, the parameters of linearized model). These may include: cracking of concrete; yielding of steel; constitutive nonlinearity in the soil, in vibration modes where structure-soil interaction is significant; constitutive nonlinearity in specially designed vibration isolator, damper, or controller; relative movement among parts meeting at structural joint; or geometric nonlinearities, i.e. nonlinear force-deflection relations especially in structures or structural members that carry significant axial as well as bending and shear forces. On account of some of all of these, with increasing amplitude the effective periods often (but not always) tend to elongate, and the damping ratios to increase [e.g. Ref. 12-13]. Recall that the empirical equation for damping ratios of tall buildings given by Eq. 8, includes the displacement amplitude as a parameter. References 14 and 15 give detailed accounts of full-scale tests and identification of amplitude-dependent equivalent natural periods and damping ratios of two buildings: a 910-ft skyscraper in New York subjected to severe wind conditions [Ref. 14]; and a 43-story steel-frame building in Los Angeles subjected to a moderate earthquake [Ref. 15.].

TEMPORAL AND SPATIAL PROPERTIES OF EARTHQUAKE AND WIND

Spectra of ground acceleration and wind turbulence

In the preceeding discussion, the dynamic properties of structure were characterized by parameters that were initially assumed to be independent of earthquake or wind action. It is likewise assumed in the following that earthquake and wind properties are independent of the structure.

At any given site, time records of ground acceleration and wind velocity, which are the main physical quantities related to seismic and wind loadings, are usually very complicated (e.g. Figs. 12-13). Perhaps the only obvious contrast between two such records, is the nonzero average value of wind speed against the zero mean value of ground acceleration.

Timewise or temporal variations of such "random" data may be better appreciated when described by power spectral density functions, a type of statistical function in the frequency domain [e.g. Ref. 18]. Essentially, the randomly fluctuating time record is imagined to be a superposition of many sinusoids of different frequencies (or periods), each sinusoid with its corresponding average amplitude. Those frequencies whose corresponding sinusoids have relatively large respective mean amplitudes are said to be dominant.

In Fig. 14(a), a deterministic (i.e. not random) periodic function is described as a superposition of two sinusoids with frequencies f_1 and $f_2 = 2f_1$, where the deterministic amplitude of the highest-frequency sinusoid is half that of the other sinusoid. In Figs. 14(b) and 14(c), sample time records of random data are shown together with corresponding power spectral density functions. The area under the curve of power spectral density versus

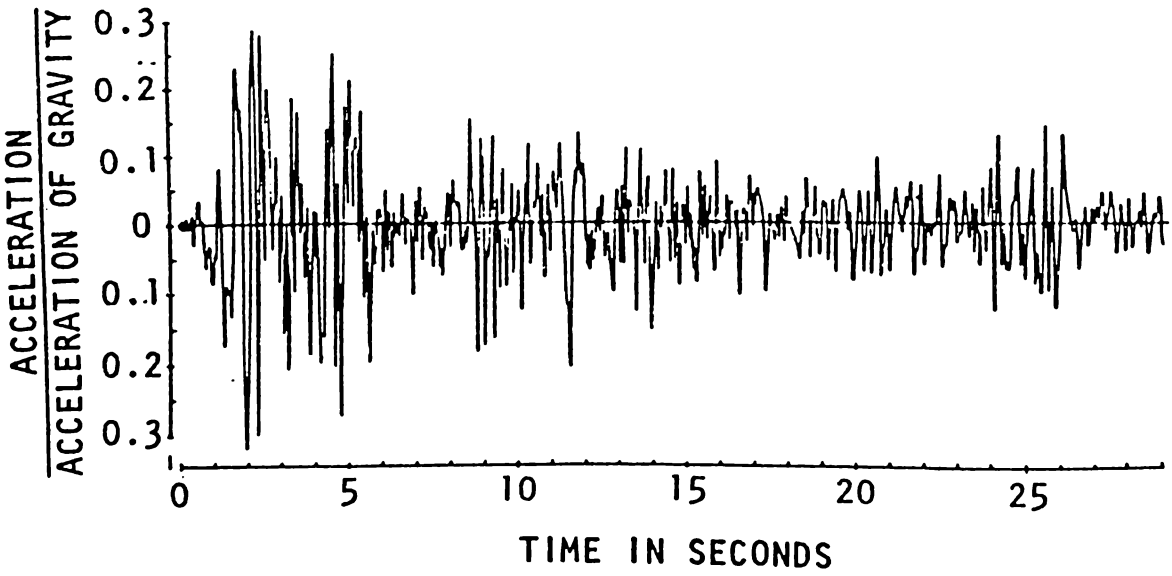

Figure 12. North-south component of ground acceleration recorded at El Centro during the El Centro, California earthquake of May 18, 1940 [Ref. 16]

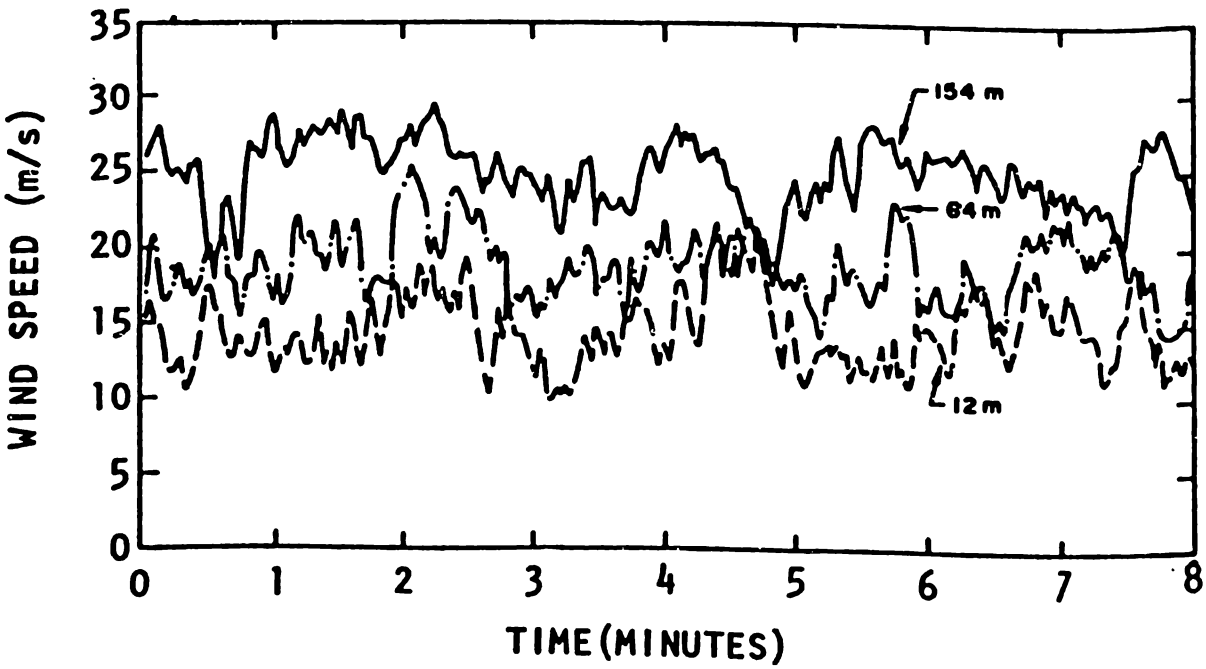

Figure 13. Wind speed at three heights on a tall mast in open terrain, East Scale, Australia [After Deacon, as quoted in Ref. 17] (Note difference in time scale compared with Fig. 12).

frequency, is equal to the mean of squared value of the random variable. Aside from this interpretation, the power spectra also shows the dominant frequencies, if any -- at such frequency, the power spectrum curve exhibits a peak. When one such frequency is highly

dominant, the spectrum looks like a narrow-band spike; and the sample time record looks nearly sinusoidal. Conversely, very random time records (e.g. Figs. 12-13) are associated with wide-band spectra as in Fig. 14(c).

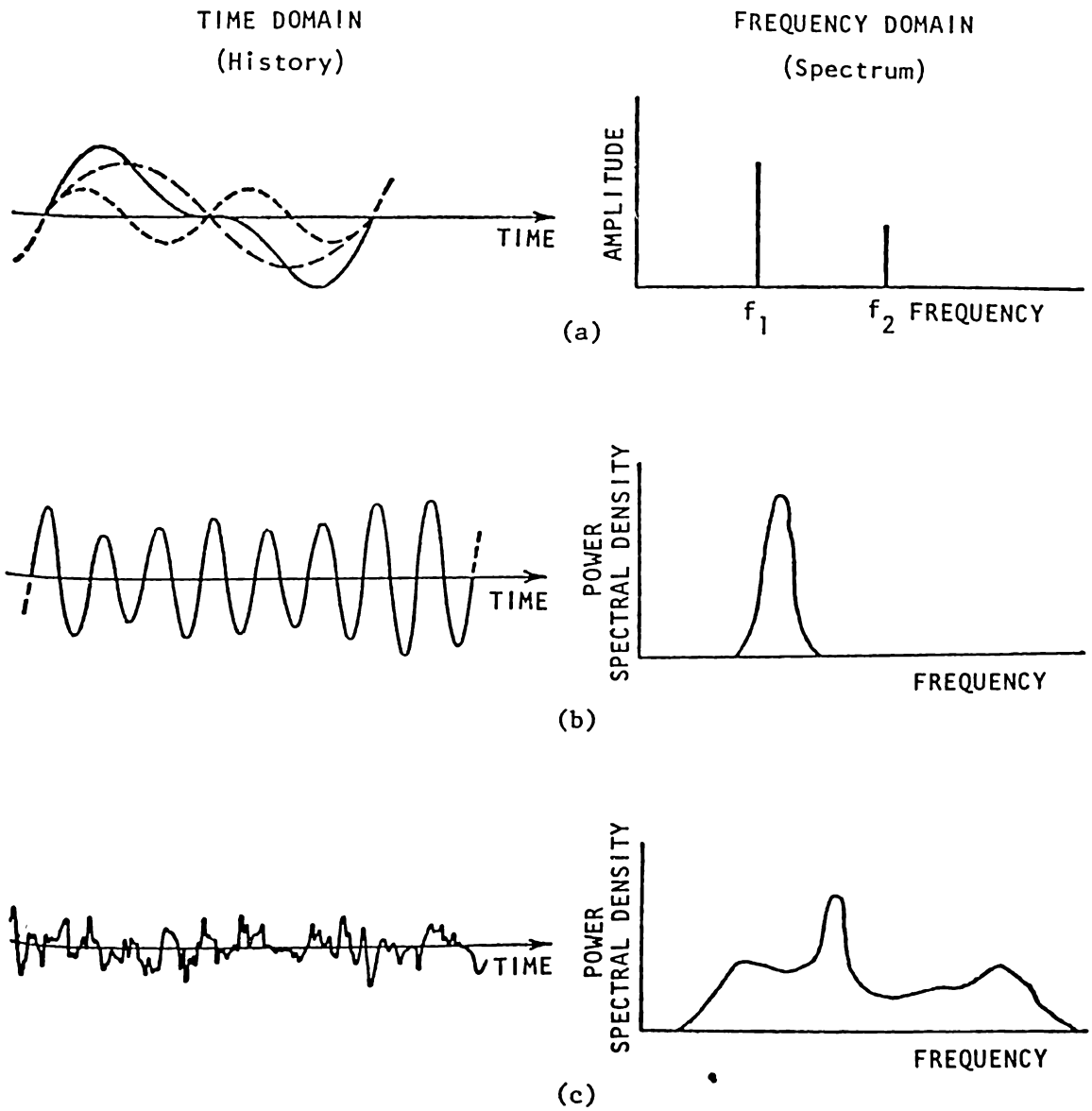

Figure 14. Hypothetical examples of zero-mean time records and corresponding frequency spectra. (a) Superposition of two sinusoids with different frequencies f_1 and f_2 and unequal amplitudes. (b) Superposition of several sinusoids with respective frequencies clustered within a narrow band around a dominant frequency. (c) Superposition of sinusoids with respective frequencies spread on a rather wide band that includes a "dominant" frequency.

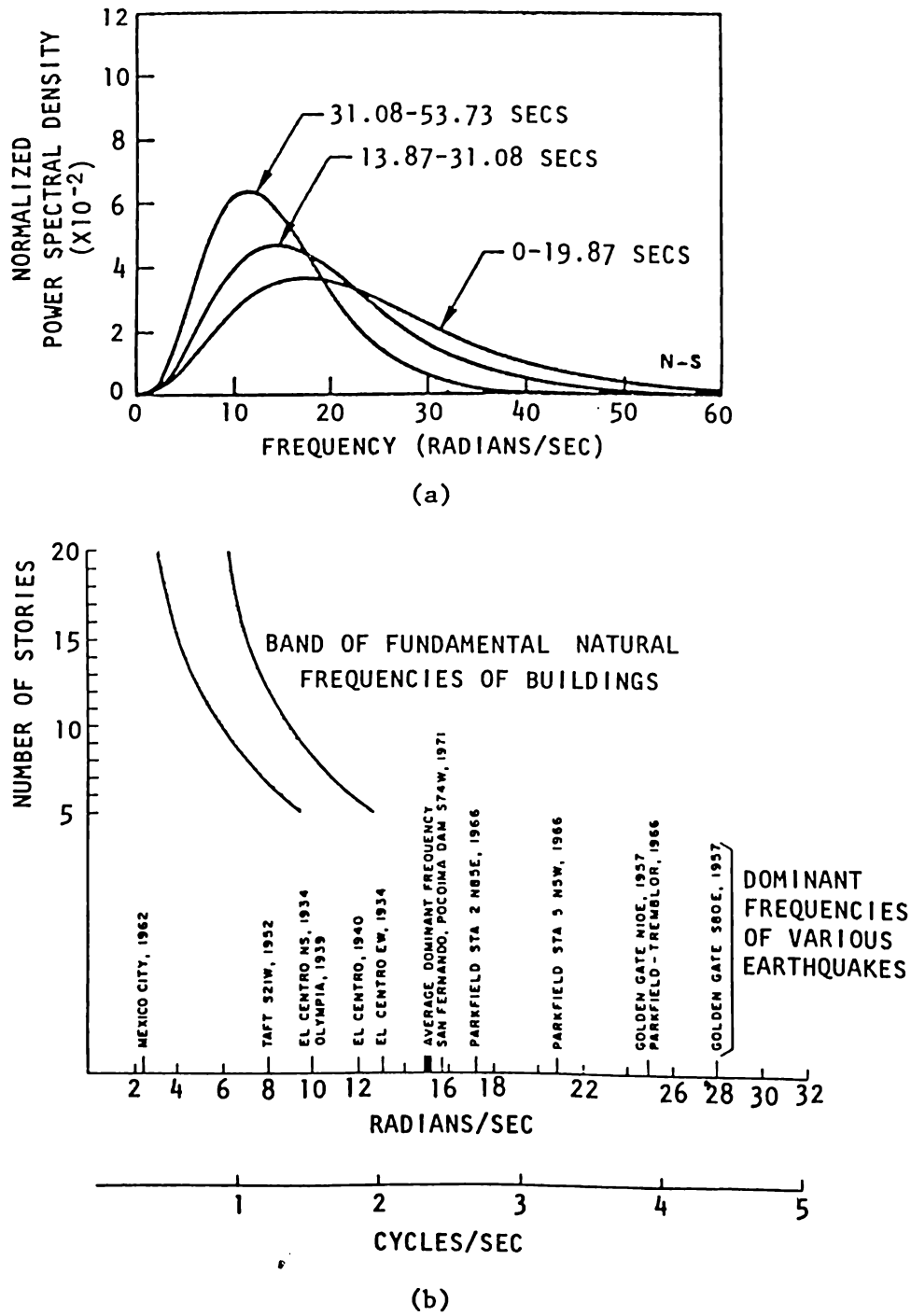

Figure 15. Coincidence of structural resonant frequencies and dominant frequencies of ground accelerations. (a) Power spectra of the NS component of 1940 El Centro earthquake (Fig. 12) as evaluated using three different segments of the time record [Ref. 19], showing a "dominant" frequency of about 2 cycles per second. (b) Dominant frequencies of some US earthquakes compared with fundamental frequencies of multi-story buildings [Ref. 20]. (Note difference in frequency scales between (a) and (b).

The power spectral density corresponding to the ground acceleration record in Fig. 12, is shown in Fig. 15(a). In fact three spectra curves are given, each one based on the processing (i.e. transformation from time domain to frequency domain) of a different segment of the accelerogram (Fig. 12) and normalized such that the area under each curve is equal to the same constant. The differences in the spectra reflect the nonstationarity of the ground acceleration as a random process; the statistics describing the variable acceleration are changing with time. Nevertheless, it can be seen that the dominant frequency of this ground acceleration is about 2 Hz. Equivalently, the sinusoid with most power has a period of about 0.5 second per cycle.

In Fig. 15(b), the average dominant frequency of several strong ground accelerations recorded in the US is shown to be about 2.5 cycles per second, higher than the usual fundamental frequencies of multi-story buildings;. Coincidence of dominant ground acceleration frequency and fundamental structural frequency would be more likely in low-rise or short-period structures. For high-rise buildings and other structures with comparably long natural periods, the dominant ground acceleration frequency may be comparable with the frequencies of the higher modes instead of with the fundamental modes.

NOTE : Two different ways of presenting power spectral densities.

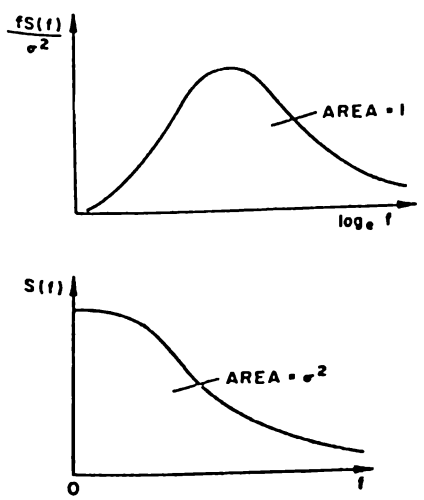

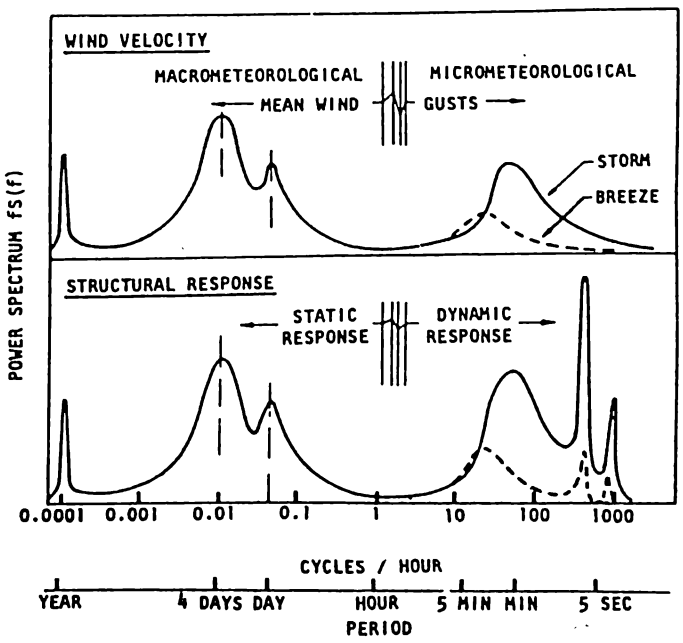

Figure 16. Idealization of the wind speed spectrum over an extended frequency range [After van der Hoven] and corresponding spectrum of structural response [After Davenport], showing range where structural response is dynamic [Ref. 17] (Note that the frequency scale is different from Fig. 15(a), and that the vertical ordinate is spectral density multiplied by frequency.)

In contrast with ground acceleration, it is often sufficient to consider wind speed fluctuation as a stationary random variable, i.e. with time-invariant statistics including power spectral density. An idealized wind speed spectrum over an extended frequency range is shown in the upper portion of Fig. 16, where it is indicated that fluctuations represented by sinusoids with frequencies equal or greater than about 1 cycle per half hour are relevant to the dynamic response of structures. Such fluctuations are called gusts. Slower fluctuations represented by sinusoids with periods of an hour or longer, are considered fluctuations of the mean wind speed. Referring back to Fig. 13 would show that at each height, a nonzero mean wind speed is observable in the brief interval recorded (8 minutes), and gust-type fluctuations take place about this mean.

The gust-type fluctuation about the mean wind speed is referred to as turbulence. The power spectral density function of turbulence (multiplied by frequency) has the general shape of the right side of the upper curve in Fig. 16. Peculiarities of typhoons and other strong winds are described in Refs. 21-22.

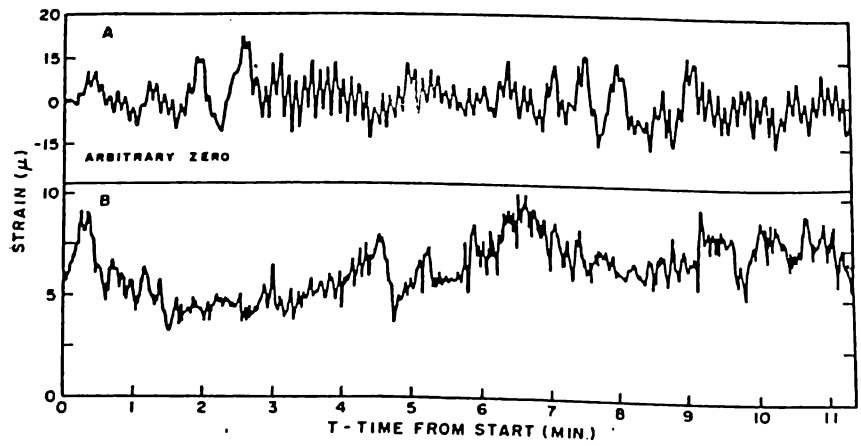

(a)

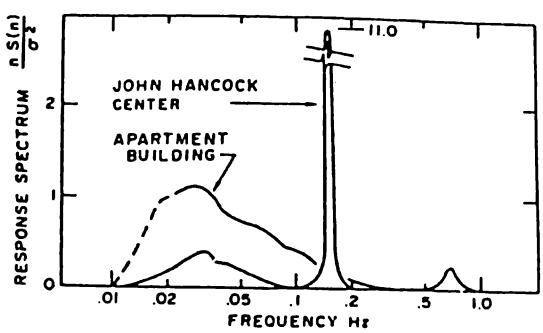

(b)

Figure 17. Comparison of wind-induced column strains in 60-story John Hancock Center skyscraper in Chicago, USA (A) and 18-story apartment building in Delft, Netherlands (B). (a) Time records. (b) Spectra, showing predominance of a resonant frequency in the case of the skyscraper. [Ref. 17.]

Figure 17 illustrates the effect of coincidence of some "power-rich" frequencies of the turbulence spectrum with natural frequencies of structure. Structural response in the form of column strain is plotted against time in Fig. 17(a), for two structures with very different natural frequencies. In Fig. 17(b), so-called reduced power spectra of the two time records are plotted using a frequency scale similar to that of Fig. 16 and vertical scale normalized by the mean squared value of the variable (i.e. strain). The response of the tall slender building displays a strong resonant character, i.e. strong dominance of the sinusoid with frequency equal to the fundamental natural frequency (between 0.1 and 0.2 Hz), as this frequency is within a relatively power-rich range in the turbulence spectrum. The response of the medium-rise building, whose fundamental natural frequency is just under 1 Hz, does not have as prominent a peak in the spectrum, since 1 Hz is relatively power-deficient in the turbulence spectrum.

From the above discussion of power spectra of wind turbulence and ground acceleration, it is noted that wind turbulence is power-rich in frequencies that are low compared to the natural frequencies of medium-rise buildings, while ground acceleration is power-rich in frequencies higher than those natural frequencies. Or, equivalently, wind turbulence is more likely to have resonant effects on high-rise or long-period structures; while ground acceleration is more likely to have resonant effects on low-rise or short-period structures. Coincidence of relevant periods is summarized in Fig. 18.

Duration and stationarity

Both from analysis and design viewpoints, the duration of strong ground acceleration or strong gusty wind at any given site, is another significant temporal characteristic in addition to power spectrum. As mentioned above, wind turbulence is often modelled as stationary process,

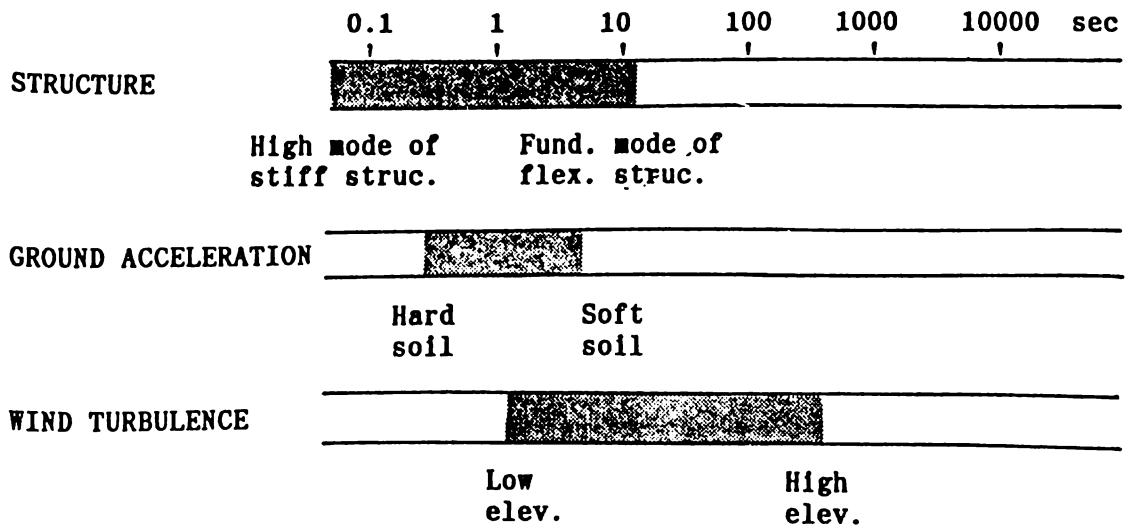

Figure 18. Common or dominant periods of oscillation or fluctuation

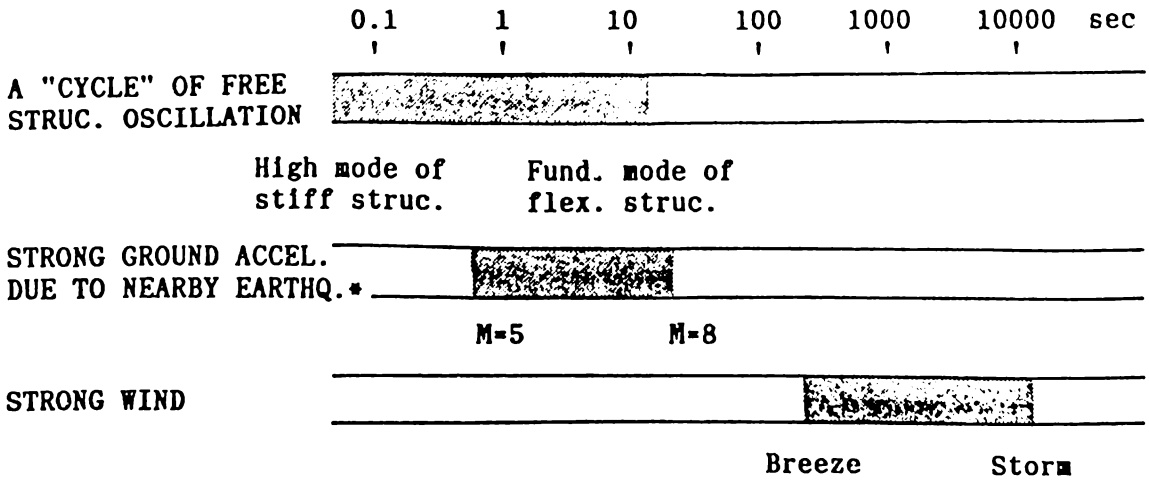

Figure 19. "Typical" durations [*Ref. 16]

i.e. with statistical properties that stay constant within the time duration of interest (e.g. duration of structural vibration). Strong ground acceleration, on the other hand, comes more as a brief shock rather than a steady excitation. A usual ground accelerogram has a short duration in the sense of Fig. 19, and has clearly defined beginning and end; hence it underlying random process is more realistically modelled as nonstationary.

Figure 19 gives a simplified graph of relevant durations which should be compared for length (rather than coincidence as in Fig. 18). From the point of view of design, long-duration actions due to strong wind are associated more with problems of serviceability and structural fatigue. Transient extreme actions due to strong ground acceleration are more associated with problems of local failure and total collapse.

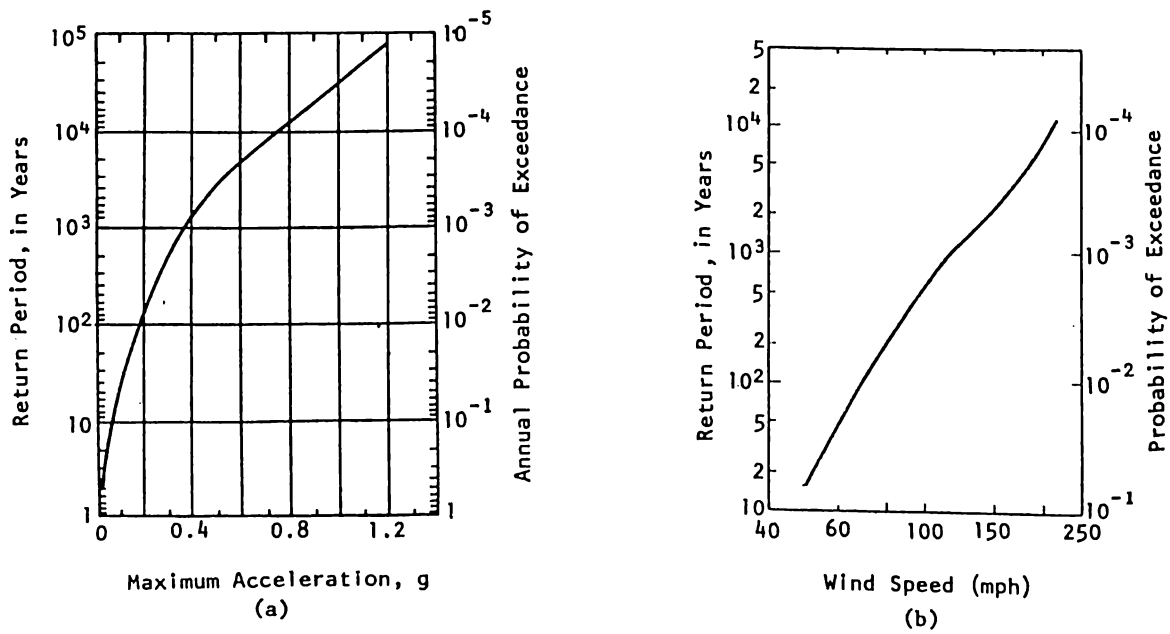

Figure 20. Return periods. (a) Ground acceleration. (b) Wind speed [Ref. 23]

Recurrence interval

A third important temporal property of ground motion or wind is its expected recurrence interval at the site. Depending on whether this mean recurrence interval is long or short compared to the intended lifetime of the structure, the structure may be or have been designed to behave either lineary or nonlinearly during each occurence of disturbances.

Figure 20 gives some idea of the return period or mean recurrence interval as function of peak ground acceleration or mean wind speed, although such functions may be highly site-dependent. An obvious trend is that higher intensity winds or ground motions have longer return periods. Although it is difficult to identify what ground acceleration and what wind speed would be "equally strong", the figure gives an impression that "major" earthquakes would have longer return periods than "severe" winds, It is in fact near-universal philosophy in aseismic design to allow significant local damage (hence structural nonlinearity) during a major earthquake, provide the probability of total collapse is acceptably small. It is deemed unreasonably expensive to design a structure to stay undamaged (hence linear) during an extreme disturbance that is only remotely possible.

Spatial properties

The site occupied by an actual structure is not a single point in space but a finite volume, and this fact may become significant as both earthquake and wind actions have characteristics that are non-uniform in vertical and horizontal directions. Explicit modelling of such two- or three-dimensional effects may be essential in the case of very tall, long or otherwise large structure. Neglect of spatial non-uniformity of earthquake or wind action may result to either conservative or unsafe design. (For further discussion, see Ref. 1 and references thereof).

STRUCTURE-MEDIUM INTERACTION

Kinematic and kinetic interactions

The discussion so far has also tacitly assumed that the dynamic response of the structure may be determined uniquely after a prior complete description of the relevant earthquake or wind environment. Such was the assumption, for example, in the discussion of buffeting response, i.e. response to wind turbulence in the direction of the mean wind, in Figs. 16-17.

In reality there is some amount of interaction between the structure and the medium in which it is founded or immersed. This interaction determines the accelerations (from earthquake) or pressures (from wind) that are effectively imposed as loads on the structure. The particular type of interaction may become so strong that the dynamic loads and the structural motions become inherently inseparable, making it impossible to first describe the load completely and next evaluate the response uniquely.

Conceptually it is convenient to classify interaction effects into kinematic or geometrical, and kinetic or inertial. Kinematic interaction of structure and soil in an earthquake environment is exemplified by the transformation of free-field accelerations (e.g. ug in Fig. 21) into the effective accelerations (e.g. u1 in Fig. 21) that are effectively imposed on different parts of the flexible founded structure. In kinetic structure-soil interaction, the structural motion in turn affects the effective accelerations at the base or foundation, as the soil itself has flexibility and capacity to either dissipate or transmit vibratory energy away from the structure.

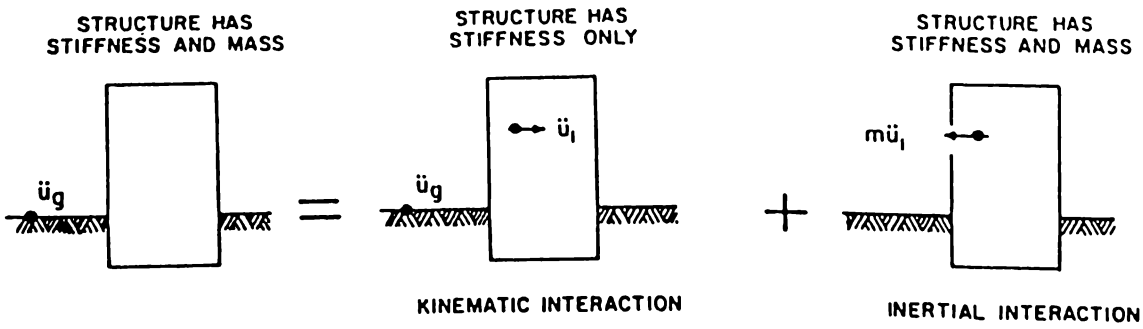

Figure 21. Two steps approach to structure-soil interaction problem in linearized model [Ref. 24]

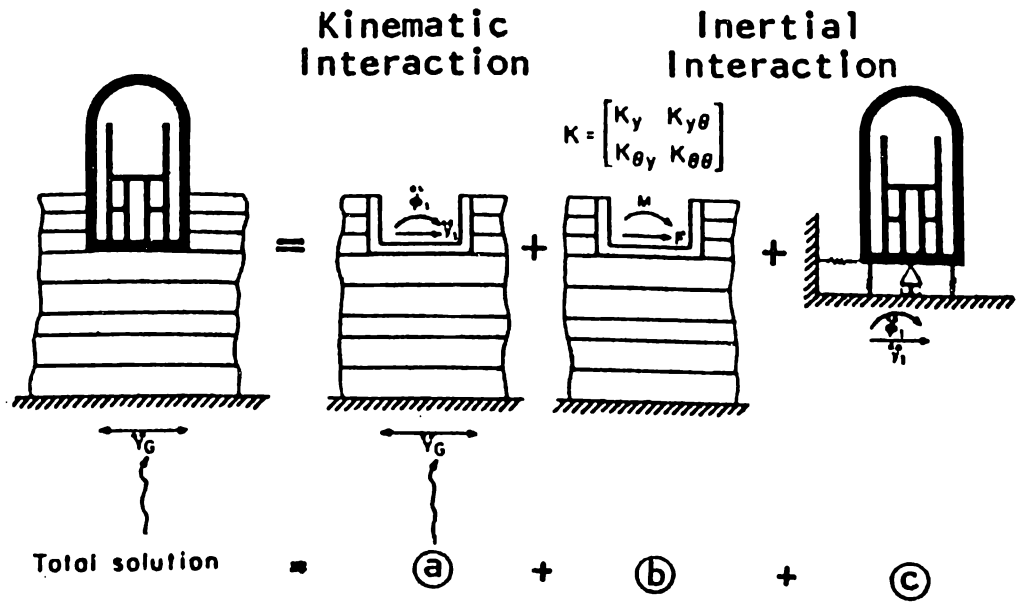

Figure 22. Three- step approach in the case of rigid foundation [After Kausel and Roesset as quoted in Ref. 24]

Kinematic interaction between structureand wind, which is traditionally the area of aerodynamics, is exemplified by the transformation of free-field wind speed and turbulence into effective pressures or suctions on the surfaces of the immersed structure. Kinetic interaction, or aeroelasticity, is when the structural motion itself significantly affects the effective aerodynamic pressures.

Structure-soil interaction

When the foundation, i.e. interface between structure and soil, is idealized to be rigid, the two-stage analysis suggested by Fig. 21 may be decomposed further into the three parts indicated by Fig. 22. The approximate kinematic interaction is the transformation of "bedrock" accelerations (e.g. yG in Fig. 23) into translational (e.g. y1) and rotational (e.g. ϕ 1) accelerations of the foundation as a unit. In kinetic interaction, these modified inputs are considered to be applied to the structure as supported by equivalent springs and dashpots (part (c) of Fig. 22). The spring and dashpot coefficients are evaluated separately as "subgrade impedance" coefficients from the following steady state relation:

$$\begin{Bmatrix} F \\ M \end{Bmatrix} e^{2\pi ft} = \begin{bmatrix} Ky & Ky\theta \\ Ky\theta & K\theta \end{bmatrix} \begin{Bmatrix} y \\ \theta \end{Bmatrix} e^{2\pi ft} \qquad (9)$$

where y is translational displacement along the axis of force F, ϕ is rocking angle about the axis of moment M, and f is frequency of steady vibration. Ky, for example, is a complex-valued quantity, the real part being associated with a spring and the imaginary part with a dashpot.

When viewed in the above manner, it is easier to appreciate the effects of structure-soil kinetic interaction not only on seismic response but also on wind-related response [e.g. Ref. 25]. Kinetic interaction generally decreases the resonant frequencies of the structure-on-flexible-soil system (part (c) of Fig. 22), compared with structure-on-rigid-ground system. Effective damping is generally increased, especially for structures that would be very lightly damped when on rigid soil.

If the foundation (interface) cannot be idealized as rigid, or when nonlinearities due to soil constitutive properties have to be explicitly considered in the seismic analysis, a direct total approach (left side of Fig. 22) may be used, where the structure and a portion of the ground are modelled as megastructure, and the ground acceleration is defined at a sufficient depth, preferably at the level of a bedrock whose acceleration could be correlated with a nearby outcrop.

All full-scale tests of actual structures inherently include structure-soil interaction. This fact must be kept in mind when using data from such tests in structure-system identification.

Structure-wind interaction

Table 4 summarizes various types of wind effects on structures. The so-called static effects are attributed to the pressures due to the mean wind which varies only very slowly compared to the natural periods of structure. More than in earthquake problem, there is a variety of wind action types.

The dynamic effects may be attributed to: 1) turbulence in the incoming wind flow, and 2) pressure fluctuations in the wake caused by the presence and oscillation of bluff body. Figure 23 shows an instantaneous picture of wind flow past bluff (i.e. not steamlined) body, illustrating the formation of fluctuating wake pressures. Forces originating at the wake are available to excite cross-wind oscillations. Thus, for given direction of mean wind, not along-wind vibrations but also cross-wind and torsional responses are generally possible.

If oscillation amplitude, either in translation or rotation, is plotted against mean wind speed , as in Fig. 24 , a classification of dynamic responses becomes practical. Classification of response according to direction of oscillation would not, however, be in one-to-one correspondence with the classification of Table 4 or Fig. 24. Along-wind response, for example, may be static or turbulence-induced. Both cross-wind response and torsional response may be turbulence-induced, vortex induced, or a form of galloping or flutter.

Table 4. Classification of wind effects on structures (Ref. 26)

<table>
<tr><td rowspan="3">Static</td><td colspan="4">Effects of time-averaged wind pressure or force</td></tr>
<tr><td rowspan="2">Instability</td><td colspan="3">Divergence</td></tr>
<tr><td colspan="3">Lateral buckling</td></tr>
<tr><td rowspan="5">Dynamic</td><td colspan="3">Turbulence response</td><td rowspan="2">Limited-amplitude response</td></tr>
<tr><td rowspan="4">Dynamic instability</td><td colspan="2">Vortex excitation</td></tr>
<tr><td>Galloping</td><td rowspan="2">SDOF flutter</td><td rowspan="3">Divergent-amplitude response</td></tr>
<tr><td>Torsional flutter</td></tr>
<tr><td colspan="2">Coupled flutter</td></tr>
</table>

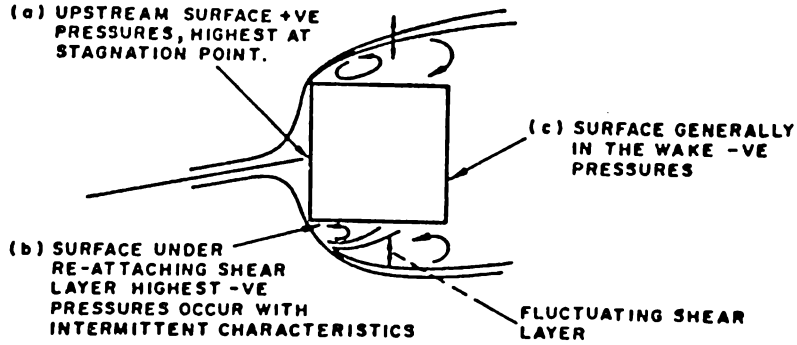

Figure 23. Three pressure areas around bluff body in turbulent wind [After Melbourne as quoted in Ref. 17]

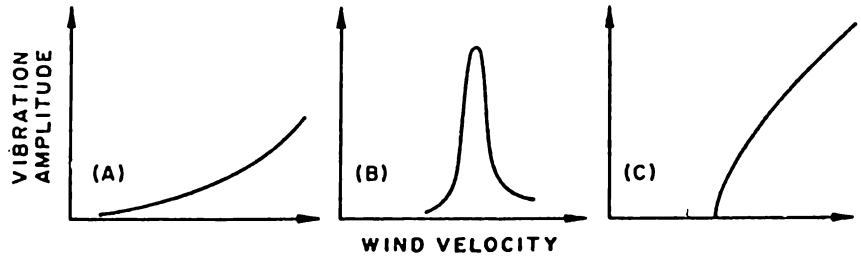

Figure 24. Main types of wind-induced oscillations of bluff structures. (a) Due to turbulence. (b) Due to vortex shedding in the wake. (c) Due to aerodynamic instability, e.g. "galloping", "flutter". [Ref. 17].

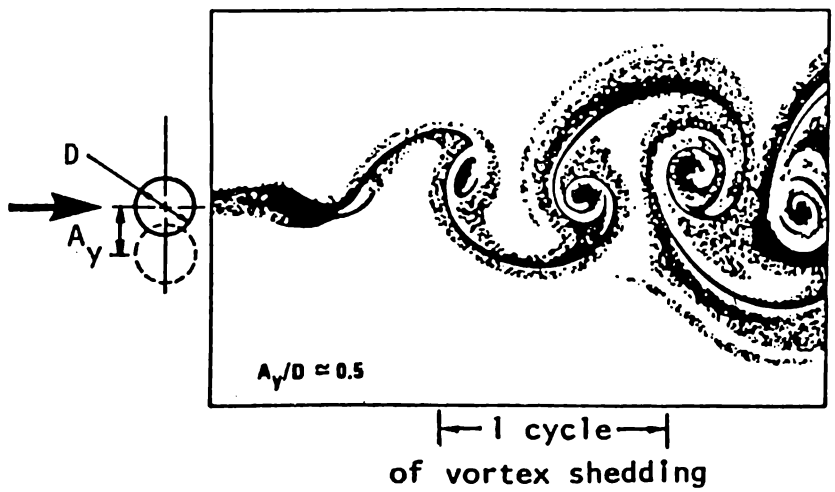

Figure 25. Vortex "street" behind an oscillating cylinder [After Griffin and Ramberg]

Among the wind-induced dynamic responses discussed above, the divergent-amplitude responses are strongly interactive. The interaction is inertial, i.e. the structural motions affect the effective wind pressures or forces. Mathematically, such oscillations are classified as self-excited, and only aeroelastic nonlinear models of analysis may predict their amplitudes.

Approximate decoupling is possible, however, not only for turbulence-induced response (as discussed above), but also for vortex excitation. The mechanism of vortex excitation is associated with a certain critical wind speed, say U_{cr}, (Fig. 24(b)) corresponding to a particular frequency of periodic shedding of vortices at alternating sides of the wake (Fig. 25). Structural oscillation becomes significant when this period of vortex shedding coincides with a natural period of structure, the phenomenon is one of resonance. The critical wind speed may be calculated as

$$U_{cr} = \frac{D}{T\,S} \qquad (10)$$

where T is structural period, D is representative dimension of the structural section, and S is the so-called Strouhal number, which depends on section shape and orientation relative to mean wind flow, and on Reynolds number which is a measure of ratio of inertia force to viscous force in the wind. At relatively low Reynolds numbers, the value of S for different sectional shapes and orientations falls mostly in the range 0.1-0.3 [e.g. Ref. 26].

In the above approach to vortex excitation, the amplitude of oscillation is to be deduced as resonant response, i.e. response to steady harmonic force with amplitude corresponding to wind speed U_{cr} and frequency equal to structural natural frequency. It may be said that the interaction is treated as kinematic. The structure section geometry, among other factors, affects the aerodynamic transformation of free-stream wind speed into a fluctuating net force in the wake, in the cross-wind direction. Essentially the section geometry screens out this force when the wind speed is not appropriate, i.e. not the critical speed.

VIBRATION CONTROL

Isolation

The remaining discussion addresses the engineer's ultimate objective: prevent unwanted vibration in his structure. First analyzed is the idea of isolation. The idea of isolating the structure from the source of vibratory energy is far from new. For example, Ref. 10 (p. 21) relates that a scientific study of earthquake-resistant building practice was undertaken in Italy shortly after the great Messina-Reggio earthquake of 1908 that killed 160,000 persons. A commission of nine prominent practicing engineers and five distinguished university professors was charged with finding methods of designing buildings that would resist earthquakes, that could be erected easily, and that would be inexpensive enough to be within the reach of the devasted population. Two contradictory proposals emerged from the commission's

deliberations. One favored isolating the building from the ground by a sand layer underneath the foundations or by supporting the building columns in the bottom story on spherical roller bearing that would permit horizontal movement. The other favored connecting the building firmly to a rigid foundation. The commission, however, adopted the latter proposal.

As for wind effects, it is fairly conventional wisdom in aircraft engineering that a body immersed in flowing wind may be considerably isolated from drag forces by proper steamlining of the cross section. Other considerations, however, have also stood in the way of straight forward application of this idea to civil engineering structures.

Of late, the general idea of isolation has been getting renewed attention from engineers who appreciate the potential advantages of "killing" the vibrations right at the source." Concepts underlying this approach are discussed below.

Seismic isolation for buildings (e.g. Fig. 26) may be interpreted approximately within a theory of linear system as follows. The introduction of base isolators serves to: 1) increase the degrees of freedom of the structure, hence increase the number of modes; 2) lower the fundamental structural frequency, presumably to push this frequency below the dominant frequency of ground acceleration anticipated at the site; and 3) increase the damping ratio of every mode in which the isolators have large deformation.

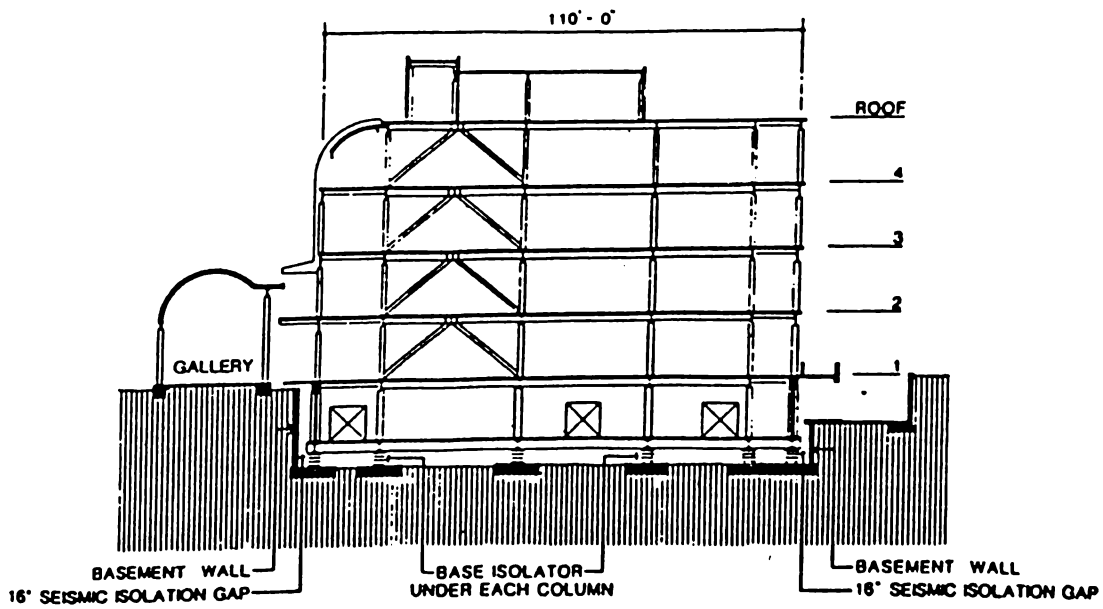

Figure 26. First base-isolated building in the US [Ref. 27, p. 251]

The actual isolators are frequently made of rubber, steel, or lead, all of which in fact have complicated and highly nonlinear force-displacement, or constitutive, properties. Many experimental studies of these isolators, both as isolated units and as installed, have recently been reported in Japan and the US. References 27-28 also give brief accounts of newly constructed base-isolated buildings and their observed performance in mild earthquakes.

Aerodynamic isolation, meanwhile, has apparently not extended from bridges to buildings. Possibly the nearest that civil engineering structures have come to aerodynamic isolation is the selection of streamlined section of bridge girder or attachment of non-structural appendages (e.g. Fig. 27). These schemes are intended to streamline the flow of horizontal wind and hence reduce the possibility of wake-induced forces. Streamlining has limited effectiveness, however, when there is significant deviation of mean wind direction from the horizontal, or when cross-wind or torsional vibration enters the picture. Considerations of aesthetics may also rule out this isolation approach. Indeed building plans are almost never laid-out with aerodynamic streamlining in mind.

Another idea of aerodynamic isolation is to expose to the wind not closed areas but perforated surfaces (e.g. Fig. 28)

Designing the structure conventionally but with a view to avoiding resonance with anticipated dynamic loads, is surely a form also of vibration isolation; but this has limited effectiveness since earthquakes and winds (and other dynamic actions) tend to have different dominant frequencies.

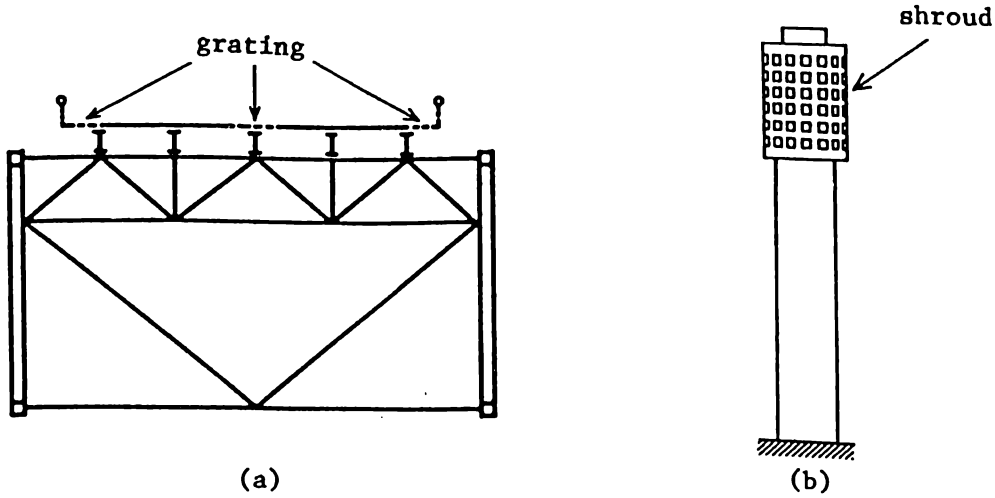

Figure 27. Aerodynamic isolators. (a) Streamlined section of bridge deck. (b) Appendages [Ref. 24]

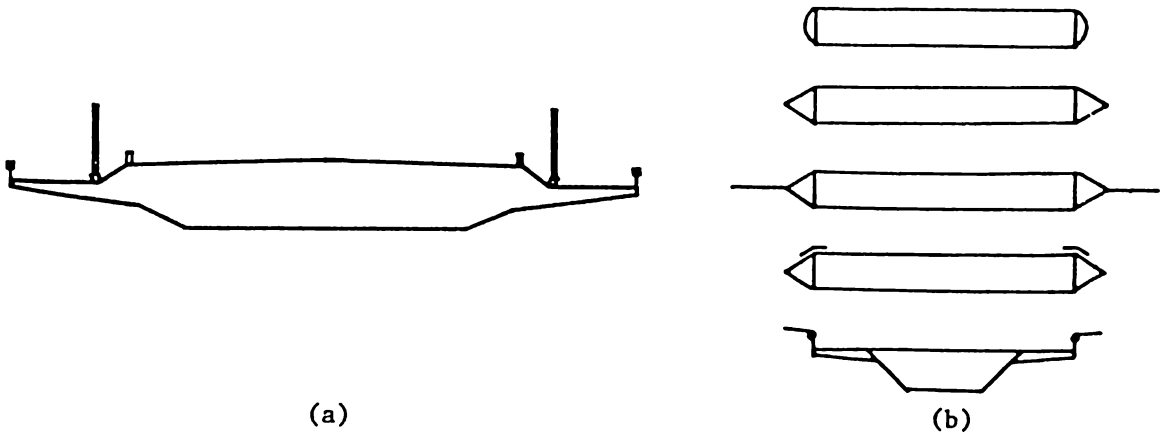

Figure 28, Aerodynamic spoilers. (a) Latticed-truss bridge girder [Ref. 24]. (b) Perforated shroud on a chimney or stack.

Table 5. Dependence of wind loads on mass, stiffness, and damping [Ref. 29]

Type of load	Design criteria	Influence of mass, stiffness and damping
Along-wind load due to turbulence	Load	Weakly dependent on $(\frac{m}{k\xi})^{0.5}$
	Accelerations	Dependent on $(\frac{1}{mk\xi})^{0.5}$
Across-wind loads on slender buildings with H/B < 6	Load	Dependent on $\frac{m}{k}\ (\frac{1}{\xi})^{0.5}$
	Accelerations	Weakly dependent on m and k Dependent on $(\frac{1}{\xi})^{0.5}$
Instability due to negative aerodynamic damping	Critical speed V_c should be beyond design range	V_c proportional to $\xi\ (m\ k)^{0.5}$
Vortex shedding	i) Crit. speed beyond design range; large amplitude motion	V_c proportional to $(\frac{k}{m})^{0.5}$
	ii) Avoidance of large amplitude motion	$\xi m > CK_a$ (where CK_a is a constant for a given geometry)
	iii) Loads due to small amplitude motion	Dependent upon $\frac{k}{m\ (\xi - \frac{CK_a}{m})^{0.5}}$

Damping

When isolation is unable to prevent vibration energy from flowing into the structure, the next logical approach in suppressing vibration is to increase the energy dissipation either in the structural components themselves or in specially attached energy absorber-dissipators.

Table 5 summarizes the roles of (modal) mass m, stiffness k, and damping ratio ξ in various wind-induced phenomena. It is indicated that an increase in damping capacity is always beneficial, whereas an increase in stiffness is not always advantageous and the correct or best choice of mass is not clear either. Reference 29 concludes that the approach of increasing the damping is "supreme if only because the inherent damping in most structures is so small that minor absolute increases in damping constitute large-proportion increases. If stresses or accelerations must be reduced significantly (e.g. by a factor of 2) then changes in mass and/or stiffness are rarely practical unless, in the case of stiffness, it is feasible to change the structural system."

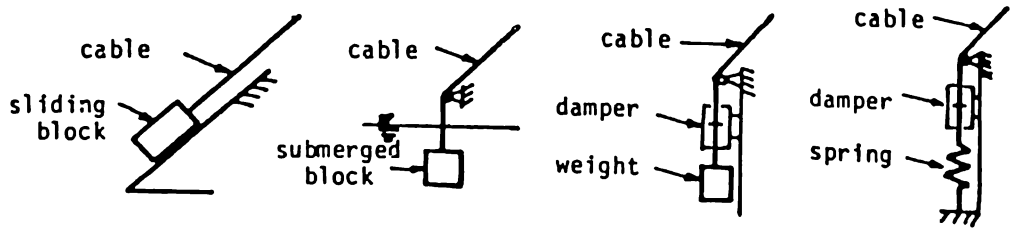

Figure 29. Examples of untuned-type passive mechanical dampers used for free-standing towers [Ref. 24]

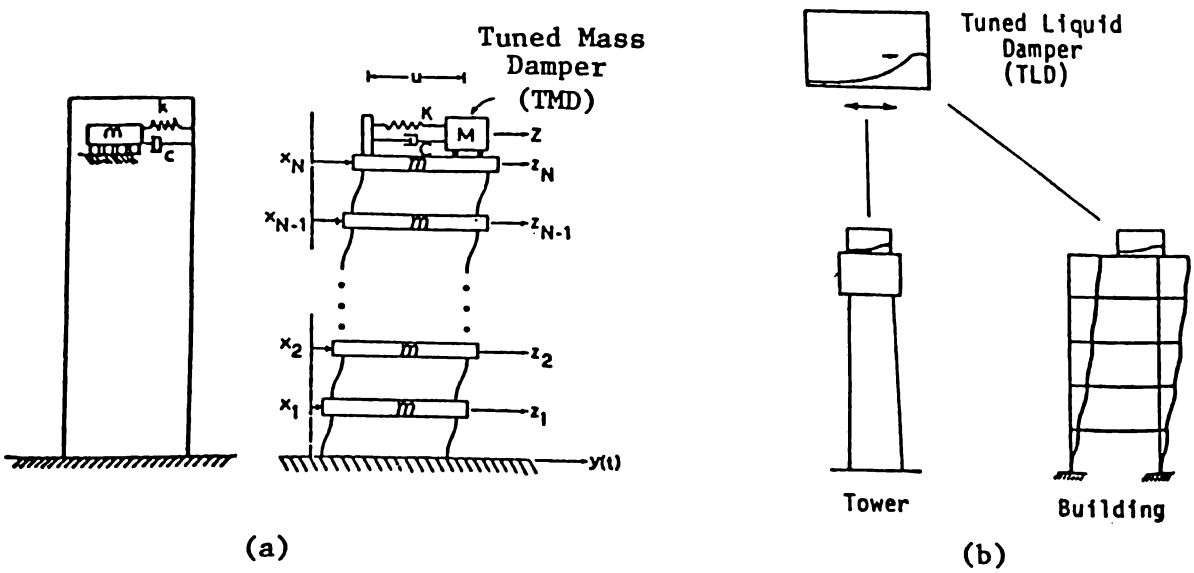

Figure 30. Examples of tuned-type passive mechanical dampers. (a) Tuned mass damper. (b) Tuned liquid damper (TLD), not to scale.

Some mechanical means of increasing the effective damping of structures, especially those already designed or constructed, are illustrated in Fig. 29-30. The so-called Tuned Mass Damper is actually an auxiliary solid mass attached to the main structure with spring-like and dashpot-like components. Reference 14 presents a detailed description of the design and performance of a 410-ton concrete mass block that was installed as TMD at the 63rd floor of a tall office building. This TMD is about 2% of the modal mass of the building in fundamental sway mode, a "typical" mass ratio. The corresponding modal damping ratio has been increased from about 0.9% to a total level higher than 4%, which is a tremendous benefit if one considers resonance excitation (Fig. 8 and Eq. 6).

Newly developed Tuned Liquid Dampers (TLD), if properly designed, are expected to better cope with some of the practical problem areas in TMD application, e.g. space requirement and installation details [Ref. 30]. However, tune-typed dampers generally tend to be less effective with random transient vibration (e.g. brief earthquake) than with harmonic steady-state vibration (e.g. prolonged wind).

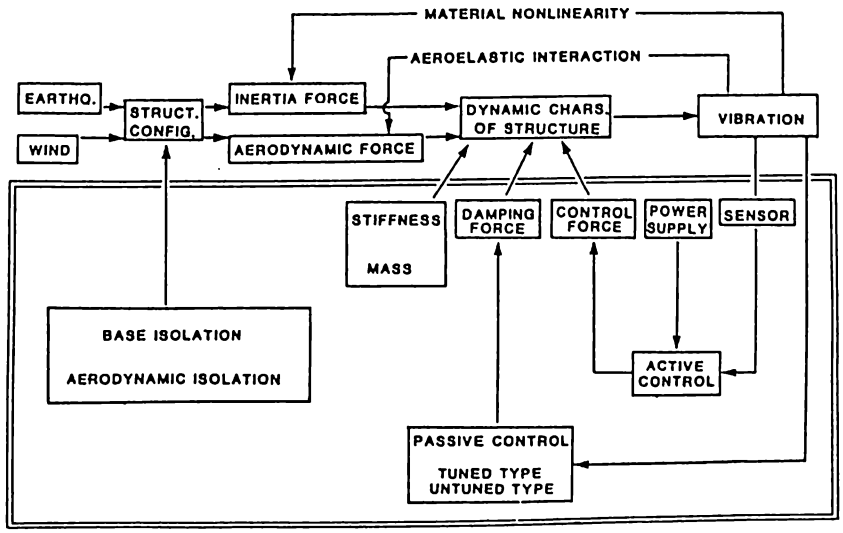

Figure 31. Measures to suppress earthquake - and wind-induced vibrations

Structural materials and components with high built-in damping capacity have also been developed. Reference 31 reviews the characteristics of various systems for vibration reduction in tall buildings, including such untuned-type viscoelastic dampers.

Active control

Figure 31 is a summary of currently recognized means of suppressing structural vibrations. "Active control," in present definition (e.g. Ref. 32), differs from the other approaches in that it involves on-site monitoring of the actual vibration and applying time-varying forces at selected points in the structure in order to counteract the other dynamic forces. This approach is perhaps the most sophisticated conceptually, and, at the same time, technologically most demanding.

CONCLUSION

The practicing engineer might dismiss all these complexities of dynamic analysis, and stick to his design codes, which can make it appear that the panacea for the headaches due to dynamic forces has been discovered. The codes, for most cases, artfully prescribe to replace these vibratory forces with easier-to-visualize and easier-to-handle "equivalent" static forces or pressures, and to design the structure statically. Yet, for structural schemes that are more creative than standard, the engineer's best design tools include the principles of applied structural dynamics.

REFERENCES

PACHECO, B. M., 1988, "Elements of Structural Dynamics in Earthquake and Wind Engineering," *Proc. Intl. Struct. Eng. Conv.*, ASEP, Manila, May

HUDSON, D. E., 1970, "Dynamic Tests of Full-Scale Structures," *Earthquake Engineering*, R. L. Wiegel (ed.), Prentice-Hall, pp. 127-149.

HART, G. C. and J. T. P. YAO, 1977, "System Identification in Structural Dynamics," *J. Eng.* Mech. Div., ASCE, Vol. 103, No. EM6, pp. 1089-1104.

NATKE, H. G. and J. T. P. YAO, 1986, "Research Topics in Structural Identification," *Dynamic Response of Structures*, G. C. Hart and R. N. Nelson (eds.), ASCE, pp. 542-550

CHOPRA, A. K., 1981, *Dynamics of Structures - A Primer*, EERI

NEWMARK, N. M. and E. ROSENBLUETH, 1971, *Fundamentals of Earthquake Engineering*, Prentice-Hall

WEAVER, W. and P. R. JOHNSTON, 1987, *Structural Dynamics by Finite Elements*, Prentice-Hall

BUHARIWALA, K. J. and J. S. HANSEN, 1988, "Construction of a Consistent Damping Matrix," *J. App. Mech.*, ASME, Vol. 55, pp. 443-447

BELIVEAU, J.-G., 1976, "Identification of Viscous Damping in Structures from Modal Information," *J. App. Mech.*, ASME, June 1979, pp. 335-339

BERG, G. V., 1983 *Seismic Design Codes and Procedures*, EERI

UMEMURA, H., M. WATABE, Y. ISHIYAMA, and T. FUKUTA, 1984, "Follow-up of New Earthquake Resistant Regulations for Buildings in Japan," *Proc. Eighth World Conf. Earthquake Eng.*, Vol. I, pp. 939-746

JEARY, A. P., 1986, "Damping in Tall Buildings - A Mechanism and A Predictor," *Earthq. Eng. Struct. Dyn.*, Vol. 14, pp. 733-750.

ITO, M., T. KATAYAMA, and T. NAKAZONO, 1973, "Some Empirical Facts on Damping of Bridges," Report 7420 presented at Symp. Resistance and Ultimate Deformability of Structures Acted on by Well Defined Loads held in Lisbon

MASCIANTONIO, A., N. ISYUMOV, and N. R. PETERSEN, 1987, "Wind-Induced Response of a Tall Building and Comparisons with Wind Tunnel Prediction," *Dynamics of Structures*, J. M. Roesset (ed.), ASCE, pp. 810-825

BECK, J. L. and P. C. JENNINGS, 1980, "Structural Indentification Using Linear Models and Earthquake Records," *Earthq. Eng. Struct. Dyn.*, Vol. 8, pp. 145-160.

MUTO, K. et al, 1980, "Earthquake Loading and Response," *Tall Building Criteria and Loading*, ASCE, pp. 45-141.

DAVENPORT, A. G. et al, 1980, "Wind Loading and Wind Effects", *Tall Building Criteria* and *Loading*, ASCE, pp. 143-248

BENDAT, J. S. and A. G. PIERSOL, 1971, "Random Data: Analysis and Measurement Procedures," Wiley

SARAGONI, G. R. and G. C. HART, 1974, "Simulation of Artificial Earthquakes," *Earthq. Eng. Struct. Dyn.*, Vol. 2, pp. 249-267

FAGEL, L. W. and S. -C. LIU, 1972, "Earthquake Interaction for Multistory Building," *J. Eng. Mech, Div.*, ASCE, Vol. 98, No. EM4, pp. 929-945

ISHIZAKI, H., 1983, "Wind Profiles, Turbulence Intensities and Gust Factors for Design in Typhoon-Prone Regions," *J. Wind Eng. Indust. Aerodyn.*, Vol. 13, pp. 55-66

METHA, K. C. and J. R. MCDONALD, 1986, "Structural Dynamics in Hurricanes and Tornadoes," *Dynamics Response of Structures*, G. C. Hart and R. N. Nelson (eds.), ASCE, pp. 28-43

ANG, A. H.-S. and Y. K. WEN, 1978, "Risk and Safety Analysis in Design for Natural Hazards Protection," Proc. US-Southeast Asia Symp. on Eng. for Natural Hazards Protection held in Manila in 1977, pp. 1-17

WHITMAN, R. V. and J. BIELAK, 1980, "Foundations," *Design of Earthquake Resistant Structures*, E. Rosenblueth (ed.), Pentech Press, pp. 223-260

NOVAK, M. and L. EL HIFNAWY, 1983, "Damping of Structures due to Soil-Structure Interaction," *J. Wind Eng. Indust. Aerodyn.*, Vol.11 pp. 295 - 306

ITO, M., 1987, "Measures against Wind-Induced Vibrations of Bridges," *Bridges and Transmission Line Structures*, L. Tall (ed.), ASCE, pp. 129-139

Abstract Volume 2 Ninth World Conf. on Earthq. Eng., 1988

"Quake Tests Base-Isolated Buildings," *Civil Engineering*, ASCE, April 1988, p. 19

VICKERY, B. J., N. ISYUMOV, and A. G. DAVENPORT, 1983, "The Role of Damping, Mass and Stiffness in the Reduction of Wind Forces on Structures," *J. Wind Eng. Indust. Aerodyn.*, Vol. 11, pp. 285-294

FUJINO, Y., B. M. PACHECO, P. CHAISERI, and L. M. SUN, 1988, "Parametric Studies on Tuned Liquid Damper (TLD) using Circular Containers by Freed-Oscillation Experiments," *J. Struct. Eng./Earthq. Eng.*, JSCE, Vol. 5, No. 2

WIESNER, K. B., 1986 "Taming Lively Buildings," *Civil Engineering*, ASCE, June 1986, pp. 54-57

SOONG, T. T., 1988, "Active Structural Control in Civil Engineering," *Eng. Struct.*, Vol. 10 pp. 74-84.